

AMERICAN UNIVERSITY OF BEIRUT

TAU HYPERPHOSPHORYLATION: A POTENTIAL
MOLECULAR MECHANISM FOR DIABETES-INDUCED
CARDIAC DYSFUNCTION

by
NIZAR WAJDI SHAYYA

A thesis
submitted in partial fulfillment of the requirements
for the degree of Master of Science
to the Department of Anatomy, Cell Biology, and Physiological Sciences
of the Faculty of Medicine
at the American University of Beirut

Beirut, Lebanon
August 2021

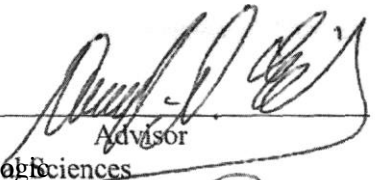
AMERICAN UNIVERSITY OF
BEIRUT

TAU HYPERPHOSPHORYLATION: A POTENTIAL
MOLECULAR MECHANISM FOR DIABETES-INDUCED
CARDIAC DYSFUNCTION

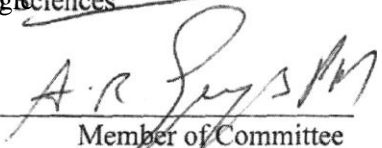
by
NIZAR WAJDI SHAYYA

Approved by.

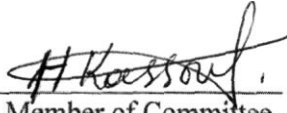
Dr. Assaad Eid, Professor
Department of Anatomy, Cell Biology, and Physiological Sciences


Advisor

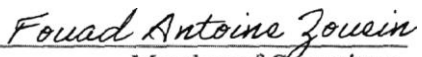
Dr. Abdo Jurjus, Professor
Department of Anatomy, Cell Biology, and Physiological Sciences


Member of Committee

Mr. Hala Kassouf, MD
Department of Pathology and Laboratory Medicine


Member of Committee

Dr. Fouad Zouein, Assistant Professor
Department of Pharmacology and Toxicology


Member of Committee

Date of thesis defense: August 30, 2021

ACKNOWLEDGMENTS

Success is based on the effort of numerous amazing people. My sincere appreciation goes to all those people who were always there to help, support, and guide me through.

First, I would like to start by extending my most genuine and heartfelt gratitude to the person who made all this possible, my supervisor and mentor Dr. Assaad Eid. Before I decided to apply for the Master's program, I held a meeting with Dr. Eid to discuss the program. His words back then were one of the main reasons I joined this program. Ever since then, his constant support, encouragement and kindness are beyond any description. Throughout these past two years, Dr. Eid was more than just a mentor, he was a friend. His guidance did not only teach me the ideal research methodology, but also how to be a better person. Words cannot express how grateful I am for what he has done for me so far, and I hope, one day, I will repay all his efforts by making him proud.

I would also like to thank the rest of my thesis committee: Dr. Abdo Jurjus, Dr. Hala Kassouf and Dr. Fuad Zoueïn for the time they spent evaluating my work.

Additionally, I would like to extend my gratitude to my fellow lab mates for all the help and support they provided me. And special thanks to Batoul, Hilda, Rachel, Natalie and Sahar for all their guidance and support throughout this journey. Without them, all of this wouldn't have been possible.

Last but not the least, no words could ever express how grateful I feel towards my number one support system, my family. I owe them absolutely everything. Without them I would have never made it this far.

ABSTRACT OF THE THESIS OF

Nizar Wajdi Shayya

for

Master of Science
Major: Physiology

Title: Tau Hyperphosphorylation: A Potential Molecular Mechanism for Diabetes-Induced Cardiac Dysfunction

Background: Diabetic cardiomyopathy is one of the major macrovascular complications of diabetes characterized by the presence of abnormal cardiac structure and performance in the absence of other cardiac risk factors. Tau protein plays a key role in microtubule assembly and stabilization, as well as cytoskeletal network modification and organization. Considerable research highlights that the accumulation of tau protein into intracellular aggregates is a pathological feature of several neurodegenerative disorders including Alzheimer's disease, Huntington's disease, progressive supranuclear palsy, etc. In addition, our group has previously shown that Tau protein plays a major role in podocyte injury. Nonetheless, its function in diabetes-associated cardiac injury remains poorly investigated.

Aim: In this study, we aim to assess the role of Tau hyperphosphorylation and aggregation in diabetes-induced cardiac dysfunction. We will also elucidate the interplay between Tau hyperphosphorylation and ROS production by the NADPH oxidases, specifically the CYP4A family of enzymes, known for its involvement in diabetic cardiomyopathy.

Methods: Type 2 diabetic rodents (mice and rats) were used. Male Sprague-Dawley rats were divided into control, T2D rats, T2D rats treated with Tau inhibitor Lithium Chloride. In parallel FVB/NJ mice were divided into control, T2D mice, and T2D mice treated with CYP4A inhibitor HET0016. Cardiac functions, histological changes, biochemical and molecular alterations were assessed.

Results: Inhibiting Tau phosphorylation with Lithium Chloride attenuated cardiac injury in the diabetic rats by significantly decreasing collagen and glycogen deposition in the heart. This was paralleled by an increase in the ejection fraction and fraction shortening %. Moreover, inhibiting Tau hyperphosphorylation attenuated ROS production and regulated the NADPH oxidase activity. Of interest, inhibiting 20-HETE production in diabetic mice using HET0016 modulated Tau phosphorylation and reversed diabetic cardiomyopathy, suggesting a potential crosstalk between Tau hyperphosphorylation and 20-HETE overproduction.

Conclusion: Our results suggest that Tau/NADPH axis plays a pathogenic role in diabetes-induced cardiac dysfunction. Collectively, inhibiting either Tau phosphorylation or CYP4A-induced 20 HETE overproduction attenuates cardiac injury.

TABLE OF CONTENTS

ACKNOWLEDGMENTS	1
ABSTRACT	2
TABLE OF CONTENTS	3
ILLUSTRATIONS	5
TABLES	6
ABBREVIATIONS	7
INTRODUCTION	0
A. Diabetes and diabetic complications: Diabetic Cardiomyopathy	0
B. Oxidative stress	1
C. Oxidative stress in diabetic cardiomyopathy	2
D. Cytochrome P450	3
1. Cytochrome P450 metabolite: 20-HETE	4
2. Cytochrome P450: a source of ROS in DCM	4
E. Tau protein	5
1. MAPT gene	6
2. Tau protein structure	8
3. Tau protein function	10
4. Post-translational modifications: hyperphosphorylation	12
5. Tauopathies	14
6. Tau in tissues: Heart	14
F. Aims and Hypothesis of the Study	16
MATERIALS AND METHODS	17

A. Animals and Treatment.....	17
B. Echocardiographic assessment	18
C. LV histology	19
D. Detection of intracellular superoxide in LV tissue using HPLC	19
E. Western Blot Analysis	20
F. Statistical Analysis.....	21
RESULTS	22
A. Alteration in Tau hyperphosphorylation mediates hyperglycemia-induced cardiac injury	22
B. Treatment with LiCl attenuates ROS production	27
C. Inhibition of 20-HETE regulates diabetes induced cardiac injury	28
D. Inhibiting 20-HETE production modulates Tau hyperphosphorylation.....	31
DISCUSSION.....	33
LIMITATIONS AND FUTURE PERSPECTIVES	40
REFERENCES	41

ILLUSTRATIONS

Figure

1.	MAPT gene and the isoforms produced upon alternative splicing.....	8
2.	Tau protein structure.....	10
3.	Paper clip conformation of Tau protein.....	10
4.	The effect of LiCl on Tau protein hyperphosphorylation in the hearts of T2D rats.....	23
5.	The effect of LiCl on cardiac function.....	25
6.	The effect of LiCl on the histology of the LVs in the diabetic rats.....	26
7.	The effect of LiCl on ROS production in the hearts of T2D rats.....	27
8.	The effect of HET0016 on cardiac function.....	30
9.	The effect of HET0016 on the histology of LVs in T2D mice.....	31
10.	The effect of HET0016 on Tau protein hyperphosphorylation in the hearts of T2D mice.....	32

TABLES

Tables

1.	Metabolic parameters of the four groups: control rats, T2D rats, and LiCl every day and every other day treated T2D rats	24
2.	Metabolic parameters of the three groups: Control+HET0016, T2D, and T2D+HET0016.....	29

ABBREVIATIONS

20-HETE	20-Hydroxyeicosatetraenoic Acid
AD	Alzheimer's Disease
AGEs	Advanced Glycation End Products
APP	Amyloid Precursor Protein
CBD	Corticobasal Degeneration
CNS	Central Nervous System
CYP	Cytochrome P450
DCM	Diabetic Cardiomyopathy
EF	Ejection Fraction
FPN	Ferroportin
FS	Fraction Shortening
GSK-3 β	Glycogen Synthase Kinase 3 Beta
H ₂ O ₂	Hydrogen Peroxide
KO	Knock Out
Lck	Lymphocyte-specific Protein Tyrosine Kinase
MAPT	Microtubule Associated Protein Tau
MMP	Matrix Metalloproteinase
NADPH oxidase	Nicotinamide Adenine Dinucleotide Phosphate Oxidase System
NFTs	Neurofibrillary Tangles
O ²⁻	Superoxide Anions
PAD	Phosphatase Activation Domain

PD	Pick's Disease
PHFs	Paired Helical Filaments
PKC	Protein Kinase C
PP1	Phosphatase Protein 1
PSP	Progressive Supranuclear Palsy
ROS	Reactive Oxygen Species
T1DM	Type 1 Diabetes Mellitus
T2DM	Type 2 Diabetes Mellitus

CHAPTER I

INTRODUCTION

A. Diabetes and diabetic complications: Diabetic Cardiomyopathy

The term diabetes mellitus was coined by the Greek physician Aertaeus, whereby diabetes means, “to pass through” and mellitus means honey or sweet (referring to the sweet smell and taste of patient’s urine). In the past years, diabetes mellitus has become an epidemic and now represents one of the most prevalent disorders [1]. With its global prevalence rising in adults from 4.7% in 1980 to 8.5% in 2014, diabetes is projected to affect around 640 million adults by 2040 [2, 3]. Additionally, the two major types of diabetes are: type 1 diabetes mellitus (T1DM) and the more prevalent form type 2 diabetes mellitus (T2DM). T1DM develops when the body’s immune system destroys pancreatic beta cells. As for T2DM, the pathology extends from primarily insulin resistance to an insulin secretory defect. Nevertheless, diabetes is associated with long-term damage to organs, and subsequently organs dysfunction, especially to the eyes, kidneys, heart, and blood vessels. These are known as microvascular and macrovascular complications of diabetes [4, 5]. An observational study has suggested that the complications of T2DM are very common, with half of patients with T2DM presenting with microvascular complications and around 30% with macrovascular complications [6]. The macrovascular complications affect large vessels of the circulatory system leading to a higher incidence of cerebrovascular stroke, coronary heart disease and peripheral vascular disease. This, in turn, leads to ulceration, gangrene and lower extremity amputations. On the other hand, microvascular

complications involve damage to the small blood vessels and thus contribute to diabetic neuropathy, diabetic nephropathy, and diabetic retinopathy [5-7].

Cardiovascular complications are the major cause of morbidity and mortality in patients suffering from diabetes. Most importantly is Diabetic Cardiomyopathy (DCM) which is best defined as an impairment of cardiac function leading to heart failure, due to diabetes, in the absence of hypertension or coronary artery disease [8, 9]. In its early stages, DCM is clinically asymptomatic and characterized by increased stiffness and fibrosis. The earliest manifestations are characterized by structural and functional abnormalities, which includes left ventricular hypertrophy and decreased left ventricular compliance, depicted by reduced early diastolic filling, increased atrial filling, and prolonged isovolumetric relaxation [10, 11]. These pathophysiological changes often evolve eventually to systolic dysfunction accompanied by heart failure with reduced ejection fraction. Importantly, the underlying pathological mechanisms include, but are not limited to, oxidative stress, mitochondrial dysfunction, impaired mitochondrial Ca²⁺ handling and function, inflammation, among others [10].

B. Oxidative stress

Oxidative stress has been widely accepted to play an important role in the development and progression of diabetes and its complications [1]. Oxidative Stress is explained as an imbalance between oxidants and antioxidants, resulting in an accumulation of oxidants [12]. In other words, it is when the production of oxidants such as reactive oxygen species (ROS) is greater than the body's antioxidative metabolic ability. On that note, ROS can directly damage proteins by oxidation, or alternatively,

by oxidizing lipids to reactive lipid peroxides, or by generating reactive nitrogen species from nitric oxide. Additionally, DNA is another major site damaged by ROS and mitochondrial DNA has been suggested to be susceptible to oxidative damage [13]. However, the mechanisms by which oxidative stress promotes the progression of diabetic complications remains inconclusive.

C. Oxidative stress in diabetic cardiomyopathy

It is believed that elevated oxidative stress in diabetic milieu is the final common pathway leading to cellular injury and facilitating the progression of diabetic complication. Therefore, hyperglycemia-induced oxidative stress is one of the key players in the pathogenesis of the DCM, as manifested by myocardial cell death, fibrosis, hypertrophy, abnormalities of calcium homeostasis and endothelial dysfunction [14, 15]. This contribution of oxidative stress to DCM is derived from pathogenic and metabolic intermediates, such as the formation of advanced glycation end products (AGEs), production of cytokines or peptides (like angiotensin II), among others [16, 17]. Advanced glycation plays a major role in the development of CM, via glycation of fibrinogen and albumin, which are induced by hyperglycemia [18]. This leads to oxidative stress and the release of inflammatory cytokines, which in turn increases inflammation, and promotes vascular and myocardial damage. Mediated through different signaling pathways (like MAPK and Janus Kinase), formation of AGEs in myocardial cells causes cross-linkage of collagen molecules to each other, which leads to the loss of collagen elasticity, and subsequently, the reduction of myocardial compliance. This will increase the production of ROS and promote myocardial fibrosis [18, 19]. Moreover, hyperglycemia directly triggers certain signaling pathways, that

appear to have a pivotal role in the production of ROS, such as the activation of protein kinase C and the nicotinamide adenine dinucleotide phosphate oxidase system (NADPH-oxidase). Furthermore, increased NADPH activity in cardiomyocytes is associated with an increase in the production of free radicals, leading to oxidative myocardial injury [16, 20]. Thus, NOX plays a major role in ROS production by utilizing NADPH as an electron donor to produce superoxide anions (O_2^-) and Hydrogen Peroxide (H_2O_2). These high levels of oxygen radicals lead to DNA damage at the cellular level and to mitochondrial dysfunction by inactivating mitochondrial enzymes, which in turn, will lead to myocardial injury [21].

D. Cytochrome P450

In the mid-1950s, the existence of an enzyme in the liver that was able to metabolize several drugs was reported [22]. Known to be present in all kingdoms of life, Cytochrome P450 (CYP) was subsequently identified, and a large amount of literature has since emerged [23]. Cytochrome P450 monooxygenases are a superfamily of heme-thiolate proteins, involved in the metabolism of various endogenous and xenobiotic compounds [24]. In mammals, these proteins are primarily found in hepatocytes and other cell types, where they play a major role in oxidizing steroids, fatty acids and xenobiotics, and play an important function in the detoxification and clearance of a wide variety of compounds; in addition to, hormone synthesis and breakdown, cholesterol synthesis and vitamin D metabolism [25, 26].

1. Cytochrome P450 metabolite: 20-HETE

The CYP4A subfamily of CYPs, which are highly expressed in the heart, fall under the hydroxylase subfamily of CYPs [27]. These metabolize arachidonic acid into eicosanoids, that are further metabolized into less active molecules. Of interest is 20-hydroxyeicosatetraenoic acid (20-HETE), which is physiologically active in the cardiovascular system and is involved in multiple cellular functions, whereby they mediate pathways associated with inflammation and apoptosis. 20-HETE, is a vasoactive eicosanoid and an essential component of the cardiovascular system whose effects in the vasculature are multidimensional and include sensitization of smooth muscle responsiveness to constrictor stimuli, stimulation of cell migration and proliferation, as well as activation of endothelial cell dysfunction and inflammation. These effects have significant implications regarding the pathophysiology of the cardiovascular system [28]. On that note, evidence from experimental and clinical work suggested that an increase in 20-HETE levels contribute to cardiovascular disease, manifested by hypertension, stroke and myocardial infarction, among others [28, 29]. Additionally, even though current knowledge regarding the role of 20-HETE in hypertrophic cardiac remodeling and cardiac failure is still minimal, 20-HETE levels were shown to be elevated in Ang II-induced hypertrophy of the heart, and the pretreatment with hydroxylase inhibitors to prevent 20-HETE production was partially protective against development of cardiac hypertrophy[28, 30]

2. Cytochrome P450: a source of ROS in DCM

ROS formation has gained significant experimental and clinical evaluation amongst a variety of mechanisms involved in the development of diabetic

cardiomyopathy. ROS production decreases the antioxidant capacity of the diabetic myocardium, contributing to oxidative stress and resulting in myocardial damage [31]. Additionally, this is underlined by several hyperglycemia-induced pathogenic mechanisms, such as the activation of polyol pathway, formation of AGEs, activation of protein Kinase C (PKC), etc. Interestingly, the activation of these pathways exacerbates oxidative stress [32]. Furthermore, ROS activates matrix metalloproteinase (MMP) in cardiac fibroblasts, leading to structural changes in the myocardium. This, in turn, results in structural changes in the myocardium, leading to cardiac remodeling, decrease in contractility, dysfunctional Ca²⁺ handling and eventually heart failure [21]. Moreover, a study suggests that inhibition of CYPs substantially attenuates ROS production and tissue damage after ischemia and reperfusion [31]. Data from our group and others have demonstrated the involvement of CYP families and their metabolites in the production of ROS. Additionally, CYP activated during ischemia/reperfusion is predicted to generate ROS in proximity to critical channels in sarco/endoplasmic reticulum [31].

E. Tau protein

The microtubule-associated protein Tau discovery dates back to 1975 when Weingarten et al. were investigating the factors involved in microtubule assembly and identified Tau as a heat stable protein essential in this process. It was called Tau due to its ability to induce tubulin formation [33]. The primary function of Tau protein is to maintain the complex neuronal cell microarchitecture, by stabilizing microtubules and modulating their dynamics, particularly in the axon [34] [35]. Nonetheless, intensive studies performed over these past years have shed the light over other important and

newly discovered physiological roles for Tau. The latter was originally thought to be expressed only in the nervous system, but it was shown that it was expressed in other tissues as well [36]. Additionally, the phosphoprotein tau's biological activity is regulated by the state of its phosphorylation [37]. Tau phosphorylation is important for its normal function; however, tau can be hyperphosphorylated leading to various pathological outcomes, most of which arise in the CNS. This paved the way for even more physiological and pathological roles of Tau to be identified and further investigated, not only in the brain and nervous system, but also in other tissues. The current review will be discussing the Tau protein structure and origin, as well as its physiological functions and expression in other tissues.

1. MAPT gene

The human MAPT gene is a long (134 kb) gene located on chromosome 17q21. The sequence of this gene is well conserved among mammals, which is surprising considering the specific human susceptibility to developing tauopathies [38]. Tau gene is transcribed into nuclear RNA that, by alternative splicing, produces different mRNAs. The translational of these distinct spliced mRNAs results in the generation of 6 stage and cell type-specific tau isoforms, ranging from 352 to 441 amino acids in the length, with their molecular weight ranging between 45 and 65 kDa [39]. Tau protein contains 16 exons. Exon 1 is part of the promoter and is thus transcribed but not translated. Exons 1, 4, 5, 7, 9, 11, 12, and 13 are constitutive exons [40]. Splicing of exons 4A and 6 in the peripheral nervous system gives rise to other tau isoforms called high molecular weight tau or big tau [41]. The six isoforms created are based on the splicing of exon 2, 3 and 10. These isoforms combinations are $(2^+3^+10^+; 2^-3^-10^-;$

$2^+3^-10^-$; $2^+3^+10^-$; $2^-3^-10^+$; $2^+3^-10^+$) [39, 42]. These isoforms can be categorized depending on the absence or presence of 1 or 2 amino-terminal inserts, which are encoded by exons 2 and 3, and are designated by N, and on whether they contain 3 or 4 carboxy terminal repeats, which are encoded by exons 9,10, 11 and 12, and are designated by R [43]. The N-terminal inserts are acidic in nature and are followed by a basic proline-rich domain. So, the longest form of the protein contains all 3 exons and is called 2N4R, where it contains the 2Ns coming from exon 2 and 3, and the 4R because it has the 4 repeats coming from exon 9, 10, 11 and 12. Another isoform has the exon 3 excised and is called 1N4R; and another has both exons 2 and 3 spliced called 0N4R. Regarding the remaining isoforms, they are formed by the absence of the 2nd repeat by splicing exon 10 (2N3R, 1N3R and 0N3R). This is important because differences in the expression of these six isoforms have been associated with different tauopathies. Additionally, alternative splicing affects tau protein biological activity, where the second repeat R2 (coded by exon 10) and the amino-terminal inserts N1 and N2 are particularly important since they enhance tau binding to tubulin, making 2N4R tau the most effective in promoting microtubule assembly and 0N3R the least effective [37, 44]. Moreover, the expression of Tau is regulated by the development of the CNS, since in the adult CNS, all six isoforms are found whereas in the fetal brain only the shortest isoform (0N3R) is expressed [39].

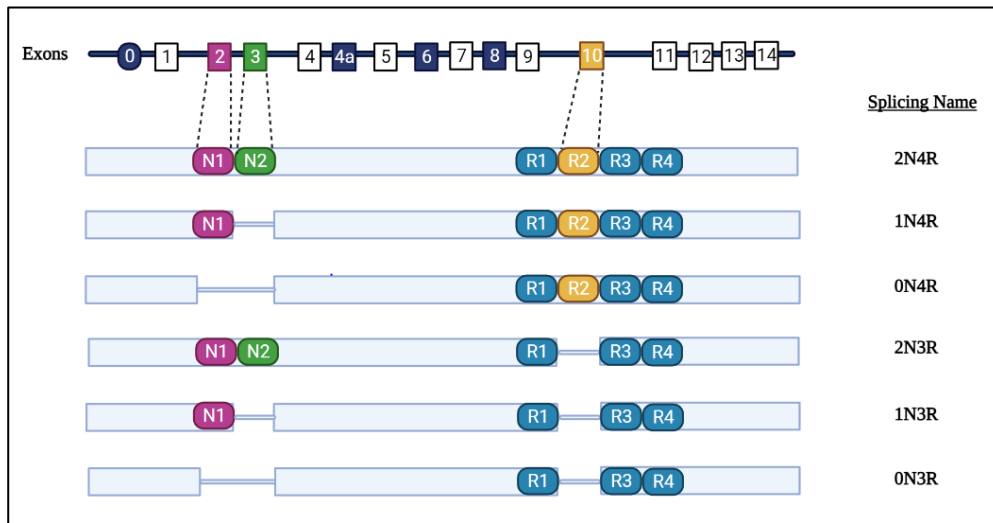


Figure 1: MAPT gene and the isoforms produced upon alternative splicing

2. *Tau protein structure*

Tau proteins are hydrophilic rod-like molecules (around 50 nm long) which bind to microtubules as periodic, short, arm-like projections [45]. The higher order structures of tau proteins have not been well identified yet, however, the primary structure can be divided into 4 functional domains, the N-terminal projection domain, a proline-rich domain, a microtubule binding domain containing four R1, R2, R3, and R4 repeats, and a C-terminal domain [46, 47].

The microtubule binding domain contains the four repeats and plays an important role in aggregation. This region contains multiple β structure elements which explains its tendency to form β structures in the aggregates [47]. Regions which are immediately before and after the microtubule binding repeat domains additionally regulate the binding of tau to microtubules. Consequently, these regions flanking the repeats are called the targeting domains and they bind strongly to microtubules but are unproductive. On the other hand, the repeats form the catalytic domain which binds

weakly, but in conjunction with the targeting domains, makes tau competent to stabilize microtubules [48].

The N-terminal projection domain protrudes from the surface of the microtubules and operates as a spacer between individual microtubules [45]. Moreover, the N-terminal domain doesn't bind microtubules directly, but is involved in regulating microtubule binding and attachment; since according to Masumoto et al., N-terminally truncated tau was harmful for microtubule assembly even in the presence of an intact microtubule binding domain. Thus, the N-terminal projection domain plays an important role in microtubule interactions [49].

The proline rich domain of tau, located upstream of the microtubule binding domain, contains seven PXXP motifs that take part in the recognition sites for SH3 containing proteins, particularly Fyn kinase. Also, residues located at the C-terminal to the PXXP motifs have been found to be able to modulate binding to the SH3-containing proteins [50] [51].

Additionally, concerning the conformation of Tau, the C-terminal tail in solution exhibits a hairpin-like structure, folding back to repeats; since, according to Jeganathan et al., the C-terminal is very close in distance to the center of the repeats. Furthermore, the N-terminal was also shown to be very close to the C-terminal end; which means that despite its natively unfolded character, tau acquires a paper-clip conformation where the C-terminal and N-terminal are brought into close proximity to each other and the repeat domain [52]. Upon binding to microtubules, the two termini of the protein are separated and the N-terminal projects away from the surface of the microtubule.

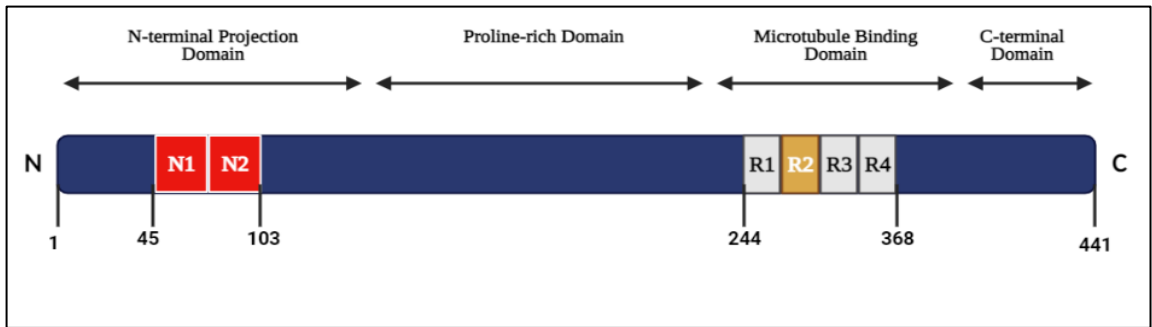


Figure 2: Tau protein structure. This structure shows the Microtubule-binding domain, the Proline-rich domain, the N-terminal, and the C-terminal

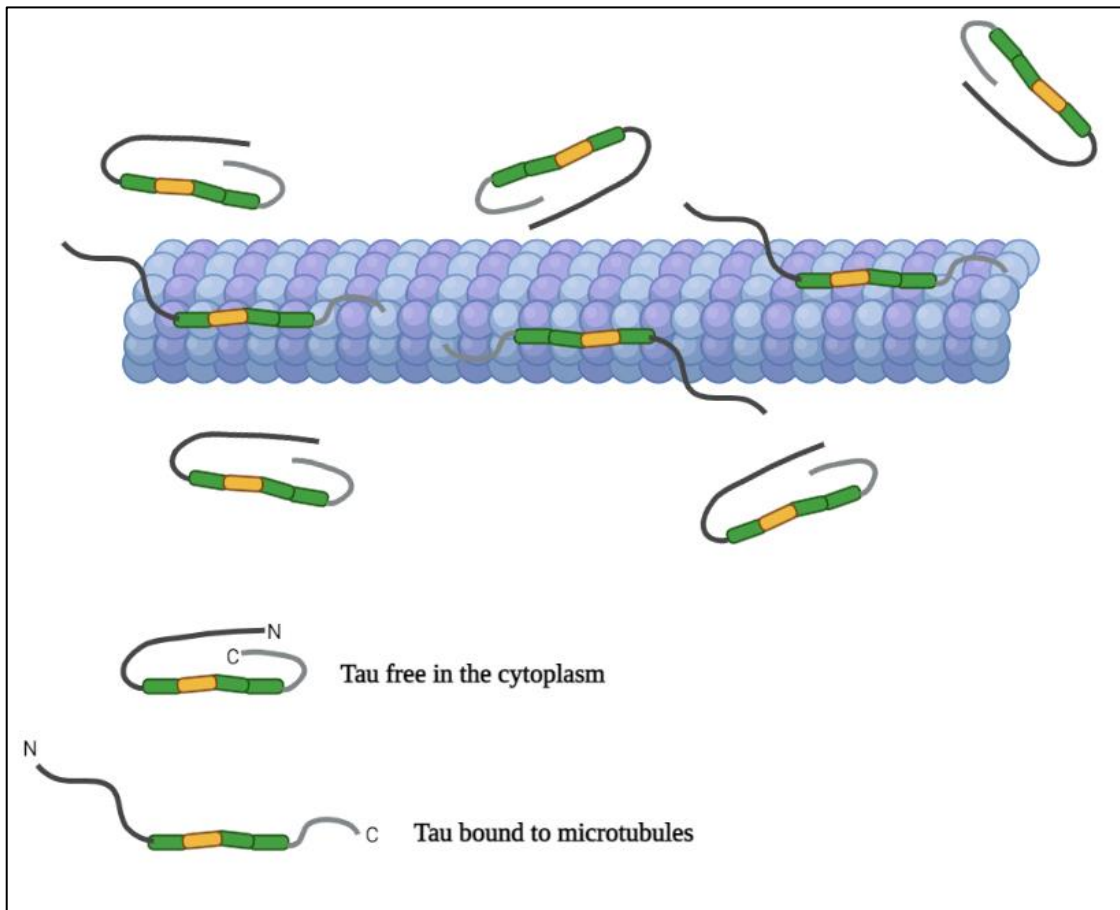


Figure 3: Paper clip conformation of Tau protein. This show the conformation of Tau protein that is free in the cytoplasm and the conformation of Tau that binds to microtubules

3. *Tau protein function*

Tau protein structure and localization are essential for its function. The main function of Tau as mentioned earlier is microtubule stabilization. Hence, Tau interacts

with the microtubules via the repeat domain and its flanking regions regulate this binding to stabilize the microtubules and to promote their assembly from tubulin subunits. It also plays a role in protecting microtubules against depolymerization by decreasing the dissociation of tubulin at both ends of the microtubule which results in an increased growth rate [35, 53]. Tau also acts as a molecular linker between actin filaments and microtubules regulating the organization of the cytoskeletal network. Thus, it plays a role in the dynamic coordination of these 2 cytoskeletons [54].

Additionally, tau regulates axonal transport by influencing the rate of attachment and detachment of motors from microtubules such that dynein-mediated movements become predominant. Hence, tau generally inhibits transport along the microtubules in the plus end direction, which leads to the accumulation of the cargoes (like mitochondria) in the somatic part of the cells overexpressing Tau protein [55].

Another role of Tau is via the PAD (phosphatase activation domain) which is found from amino acid 2 to 18 in the N-terminal region. PAD activates PP1 (phosphatase protein 1) which leads to the dephosphorylation of microtubule associated proteins, enhancing their association with microtubules, and promoting microtubule assembly and stability. This interaction is regulated via cellular signaling transduction pathways, which suggests a role of Tau in the signaling cascade by PP1 regulation [56].

Moreover, recent studies have shown that Tau protein is involved in regulating cell activity and viability. Ergo, Tau plays an antiapoptotic role in the cells by competitively inhibiting the phosphorylation of β -catenin by GSK-3 β and thus stabilizing β -catenin which leads to its translocation to the nucleus to promote cell survival and protection from apoptosis [57]. Moreover, Tau has also been shown to play

an essential role in the protection of neuronal DNA integrity. Tau nuclear accumulation preserved DNA integrity from heat stress-induced damage. This protection may be mediated through Tau interaction with the A-T-rich DNA minor groove; however, the detailed mechanism is still unknown [58].

Adding to that, Tau can also interact with members of Src-family via the proline rich domain, as mentioned earlier, such as Fyn and Lck which are important for controlling cell signaling in the neurons. Tau activates Fyn via NMDA receptors and this interaction also plays a role in process extension in oligodendrites, and in targeting Fyn to the post-synapse in the dendritic spines [59, 60].

Finally, intraneuronal iron accumulation, neuronal loss in the substantia nigra and a severe decline in locomotor functions were observed in 12-month-old tau-knockout mice. This latter observation shows that Tau deficiency can cause iron accumulation inside neurons by preventing the trafficking of APP to the cell surface, where APP usually interacts with ferroportin (FPN) to facilitate the export of iron. Notably, this accumulation of iron was observed in the brain regions with reduced soluble tau levels, such as the cortex in AD, the substantia nigra in PD and various brain regions in several other tauopathies [61].

4. Post-translational modifications: hyperphosphorylation

Tau is subject to a wide range of post-translational modifications, including phosphorylation, isomerization, glycation, nitration, acetylation, oxidation, polyamination, ubiquitylation among others [62]. Phosphorylation is the most described post-translational modification since Tau contains 85 putative phosphorylation sites,

including 45 serine, 35 threonine, and five tyrosine residues, which explains why phosphorylation has an important impact on the physiological functions of Tau [63]. Under pathological conditions, Tau phosphorylation is increased, which reduces its affinity to microtubules, and this results in cytoskeleton destabilization, particularly in neurons. Tau phosphorylation at Ser262, Ser293, Ser324 and Ser356, located in the four microtubule-binding repeats, decreases tau binding to microtubules [64]. Also, The phosphorylation of Ser214 has been implied to play a major role in the detachment of tau from the microtubules [65]. This leads to Tau detachment from the microtubules, followed by self-aggregation to form oligomers and higher order Tau aggregates [66]. Hence there is a link between abnormal phosphorylation and aggregation of Tau. Surprisingly, the tau phosphorylation in NFT was found to be very similar to a transient hyperphosphorylation of tau which occurs during development of the brain, suggesting that neurons may respond to some insult, such as oxidative stress or ischemia, with a final attempt to reenter a proliferative phase [65].

Furthermore, increased Tau phosphorylation induces neurodegeneration through mechanisms different from those described above. Thus, increased Tau phosphorylation induces its missorting from axons to somatodendritic compartments. This compromises axonal integrity and induces synaptic dysfunction [67]. Additionally, phosphorylation alters the association of Tau with its interacting partners, such as the plasma membrane, DNA and Fyn, which will leads to Tau dysfunction in many signaling pathways [63].

5. *Tauopathies*

Characterized by abnormal tau protein deposition in the brain, tauopathies are clinically, biochemically and morphologically heterogeneous neurodegenerative diseases which include, but are not limited to, AD, PSP, PD, CBD and others [68]. One particularly very important neurodegenerative disorder, AD, which is the most common form of dementia and is characterized by incremental memory loss and cognitive impairment, affects around 44 million people worldwide [69]. AD is histopathologically denoted by the formation of intracellular NFTs [70]. Tau, in the hyperphosphorylated form, forms the major molecular component of PHFs which, in turn, largely constitute NFTs, and it has been shown that all six tau isoforms are present in these inclusions [39, 71]. Tau has also been shown to be N-truncated in the process of tangle formation, and this proteolysis is as important as phosphorylation in the formation of intracellular tangles [72]. Moreover, hyperphosphorylated tau is affected by various pathological factors like aberrant activation of kinases, abnormal gene expression, chronic stress and others, leading to over-aggregation and to the formation of NFTs and thus plays a critical role in the pathogenesis of AD causing synaptic loss, impaired axonal transport, mitochondrial and cytoskeletal dysfunction, oxidative stress and other dysfunctions [73, 74].

6. *Tau in tissues: Heart*

Tau in human brain is expressed in neurons and to a lesser extent in oligodendrocytes and astrocytes [75]. It is most intensely studied in relation to its role in tauopathies, as discussed earlier. However, despite that, the pathogenesis of Tau-mediated neurodegeneration in tauopathies remains unclear.

Nevertheless, Tau protein is not only expressed in neuronal tissues. According to a study conducted by Gu Y et al., Tau exists in many non-neuronal tissues including heart, skeletal muscles, adrenal gland, testis, lung, kidney and liver. The presence of Tau protein in these tissues is not due to the translocation or transportation of Tau from the peripheral nerves, on the contrary, it is due to the presence of tau mRNA and in different proportions [36]. A study conducted by our group suggested tau hyperphosphorylation as a novel signaling mechanism involved in podocyte injury via podocyte microtubule reorganization [76]. Additionally, another study conducted by Shults et al. has shown that Tau protein is expressed in various smooth muscle tissues; specifically, the phosphorylated Tau at Threonine 181. It was also shown that Tau was expressed in a well-organized fashion, unlike most of the Tau molecules which seem to be not so organized [77]. This opens the possibility that Tau may play pathophysiological roles in the vascular system.

Concerning Tau in cardiac tissue, several studies investigated the physiological role of Tau in the cardiovascular system and explored the consequences of its loss. In the study conducted by Betrie et al., Tau KO mice showed an increased systolic blood pressure and cardiac hypertrophy; in addition to, a lower right atrial rate and a decrease in contractility [78]. Another study conducted by Rajalingam et al., explored the deletion of Tau in cardiac tissue, whereby these mice showed an increase in systolic dysfunction, a decrease in systolic and diastolic left ventricular volumes and a significant decrease in heart rate (with increased heart rate variability) indicating autonomic changes in the heart [79]. Furthermore, a study conducted on drosophila, where they investigated the expression of mutant tau, showed that tau mutation resulted

in ultrastructural abnormalities, as well as severe cardiac dilation, reduced contractility and arrhythmia [80].

Tau is an important microtubule associated protein whose function is to maintain neural structure and activity, among others. These functions are regulated by alternative splicing and post-translational modifications, most importantly of which is phosphorylation. Tau protein expression is not limited to the neuronal tissue, but it extends beyond that to reach other tissues, like the cardiac and smooth muscle tissues as discussed. However, the specific mechanisms involved in the physiology and pathology of the cardiovascular phenotype requires further investigation and thus understanding the etiopathogenesis is key for developing rational therapeutic treatments for the neurodegenerative diseases and possibly for disorders afflicting other organs like the heart.

F. Aims and Hypothesis of the Study

We hypothesize that diabetes will induce an alteration in CYP4A leading to an increase in 20-HETE production. These changes induce hyperphosphorylation of Tau in the cardiac tissue and thus its aggregation. Consequently, these molecular alterations result in inducing cardiac injury characterized by left ventricular hypertrophy, decreased fraction shortening and ejection fraction, and myocardial fibrosis via increased collagen deposition and glycosylation.

CHAPTER II

MATERIALS AND METHODS

A. Animals and Treatment

Sprague-Dawley male rats (one-month-old; 100-200 g) were randomly divided into four groups (5 animals each); Group 1-control rats were given standard chow and sodium citrate buffer injection alone. Groups 2 and 3 rats were given in-house prepared HFD (60% kcal fat) for 8 weeks and intravenously injected with 35 mg/kg body weight streptozotocin (STZ) in sodium citrate buffer (0.01 M, pH 4.5) via the tail vein to induce diabetes. Afterward, rats were divided into three groups; group 2, type 2 diabetic group, and groups 3, type 2 diabetic group that were intraperitoneally administered with 1 mmol/kg LiCl every day for 14 weeks.

In addition, FVB-Nj female mice (6 weeks old, weighing around 20 g) were randomly divided into 3 groups: Control, type 2 diabetic group and type 2 diabetic treated with HET0016 (2 animals per each group). Control mice were given standard chow; however, the other 2 groups were given in-house prepared HFD (60% kcal fat) for 4 weeks then received 3 consecutive intraperitoneal (IP) injections of 55 mg/kg body weight streptozotocin (STZ) dissolved in sodium citrate buffer (0.01 M, pH 4.5) to induce T2DM. The control group received three IP injections of sodium citrate buffer. One of the diabetic groups received 5mg/kg body weight of HET0016, a selective inhibitor for 20-HETE synthesis, administered five times a week by oral gavage for 10 weeks. The control group were given the same treatment too.

Blood glucose concentration was monitored 24 h later and weekly thereafter using LifeScan One Touch glucometer (Johnson & Johnson, United States). All rats and

mice groups were maintained in accordance with approved protocols of the Institutional Animal Care and Use Committee at the American University of Beirut. All animals were kept in a temperature-controlled room and on a 12/12-dark/light cycle and had standard chow/HFD and water access. The hearts of the anesthetized rats/mice were removed, weighed, and washed in PBS. Hearts' left ventricles were cut, snap-frozen in liquid nitrogen to be stored at -80°C for histological and biochemical analysis.

B. Echocardiographic assessment

Rat models were weighed then anesthetized using a mixture of 4:1 ketamine/xylazine, and the mice models were anesthetized using Forane. Echocardiography measurements were performed with a linear 40-8 MHz transducer (model L40-8/12, Ultrasonix Medical Corporation, Canada) connected to a high-performance ultrasound system (Ultrasonix Medical Corporation, Canada). Rats were positioned horizontally on a controlling heating pad to maintain their normal body temperature (38°C) and their anterior chest wall was shaved to place the transducer. Two-dimensional echocardiography images were obtained using M-mode and in the parasternal short- and long-axis views. LVEDD: LV end-diastolic diameter, LVESD: LV end-systolic diameter, LVEDV: LV end-diastolic volume, LVESV: LV end-systolic volume, and LVM: LV mass were measured. LV fractional shortening (FS%) and LV ejection fraction (EF%) percentages were calculated as follows: $[(LVEDD - LVESD)/LVEDD] \times 100 (\%)$ and $[(LVEDV - LVESV)/LVEDV] \times 100 (\%)$, respectively. Measurements at each time point were averaged based on six different cardiac cycles.

C. LV histology

Slices of frozen left ventricles were sectioned perpendicularly (4 μ m) for histological analysis. Myocardial fibrosis was assessed using Masson's trichrome and Periodic acid–Schiff staining. Masson's trichrome blue staining to recognize collagen deposition (37). Periodic acid–Schiff magenta staining to recognize the volume density of glycogen storage (magenta color) (38). Results were investigated under a light microscope (10x) (Olympus, CX41, Japan).

D. Detection of intracellular superoxide in LV tissue using HPLC

Cellular superoxide production in the LV was assessed by HPLC analysis of dihydroethidium (DHE)-derived oxidation products. The HPLC-based assay allows the separation of the superoxide-specific 2-hydroxyethidium (EOH) from the nonspecific ethidium. Briefly, homogenates from LV are washed twice with Hanks' balanced salt solution (HBSS)-diethylenetriaminepentaacetic acid (DTPA) and incubated for 30 min with 50 μ M DHE (Sigma-Aldrich) in HBSS–100 μ M DTPA. Tissues were harvested in acetonitrile and centrifuged (12,000 X g for 10 min at 4°C). The homogenate was dried under vacuum and analyzed by HPLC with fluorescence detectors. Quantification of DHE, EOH, and ethidium concentrations was performed by comparison of integrated peak areas between the obtained and standard curves of each product under chromatographic conditions identical to those described above. EOH and ethidium were monitored by fluorescence detection with excitation at 510 nm and emission at 595 nm, whereas DHE was monitored by UV absorption at 370 nm. The results are expressed as the amount of EOH produced (nmol) normalized for the amount of DHE consumed (i.e., initial minus remaining DHE in the sample; μ mol)

E. Western Blot Analysis

Homogenates from left ventricle isolated from the heart were lysed in 250 μ l of radioimmunoprecipitation assay buffer (0.1% sodium dodecyl sulfate, 0.5% Sodium deoxycholate, 300mM NaCl, 100 mM Tris-HCl pH 8, 1% NP-40, Protease Inhibitor Cocktail, Phosphatase Inhibitor Cocktail, and 1mM PMSF) using a Dounce homogenizer. Homogenates were placed on a rotator for 2 hrs. and centrifuged at 13,200 RPM for 30 min at 4°C to obtain a supernatant. Protein in the supernatants was measured using a Bio-Rad protein assay. For immunoblotting, proteins (60 μ g) were separated by 8% SDS-PAGE and transferred to polyvinylidene difluoride membranes. The membranes were blocked with 5% Bovine Serum Albumin (BSA) in Tris-buffered saline and then incubated with primary antibodies. The antibodies used include the rabbit polyclonal anti-Tau (phospho S214) antibody (dilution 1:250; catalog No. ab10891; Abcam, United Kingdom), the rabbit polyclonal anti-Tau (phospho S404) antibody (dilution 1:1000; catalog No. ab92676; Abcam, United Kingdom) and mouse monoclonal anti-HSC70 (B-6) antibody (1:500; catalog No. sc-7298; Santa Cruz Biotechnology, Inc., United States). The primary antibodies were detected using horseradish peroxidase-conjugated IgG (1:10000). Bands were visualized by enhanced chemiluminescence. Densitometric analysis was performed using the National Institutes of Health Image J software.

F. Statistical Analysis

Results are represented as means \pm SEM. Statistical significance is determined using one-way ANOVA, followed by Tukey's posttest. Statistical Significance was determined as a probability (P value) of less than 0.05. All statistical analyses were performed with Prism 6 Software (GraphPad Software).

CHAPTER III

RESULTS

A. Alteration in Tau hyperphosphorylation mediates hyperglycemia-induced cardiac injury

In order to examine the role of Tau phosphorylation in the pathogenesis of DCM, cardiac function was assessed by echocardiography and histological studies. The T2D rats were treated with 1mmol/kg LiCl, an inhibitor for Tau phosphorylation every day. The extent of cardiac dysfunction was evaluated by the changes in the left ventricle fractional shortening, ejection fraction and fibrosis.

To begin with, we wanted to verify the involvement of Tau hyperphosphorylation in the diabetes-induced cardiac injury. Left ventricles harvested from the 4 animal groups were used to study the protein expression. Western blot analysis results showed a predominant 79-kDa band of p-Tau ser214 which indicates an increased Tau phosphorylation in the LVs of the diabetic rats as compared to control rats (**Figures 4A and 4B**). Additionally, a significant decrease in the levels of Tau protein phosphorylation in the LV of T2D rats was observed after everyday treatment with LiCl (**Figures 4A and 4B**). Therefore, this experiment shows that tau protein hyperphosphorylation might play a role in diabetes induced heart injury.

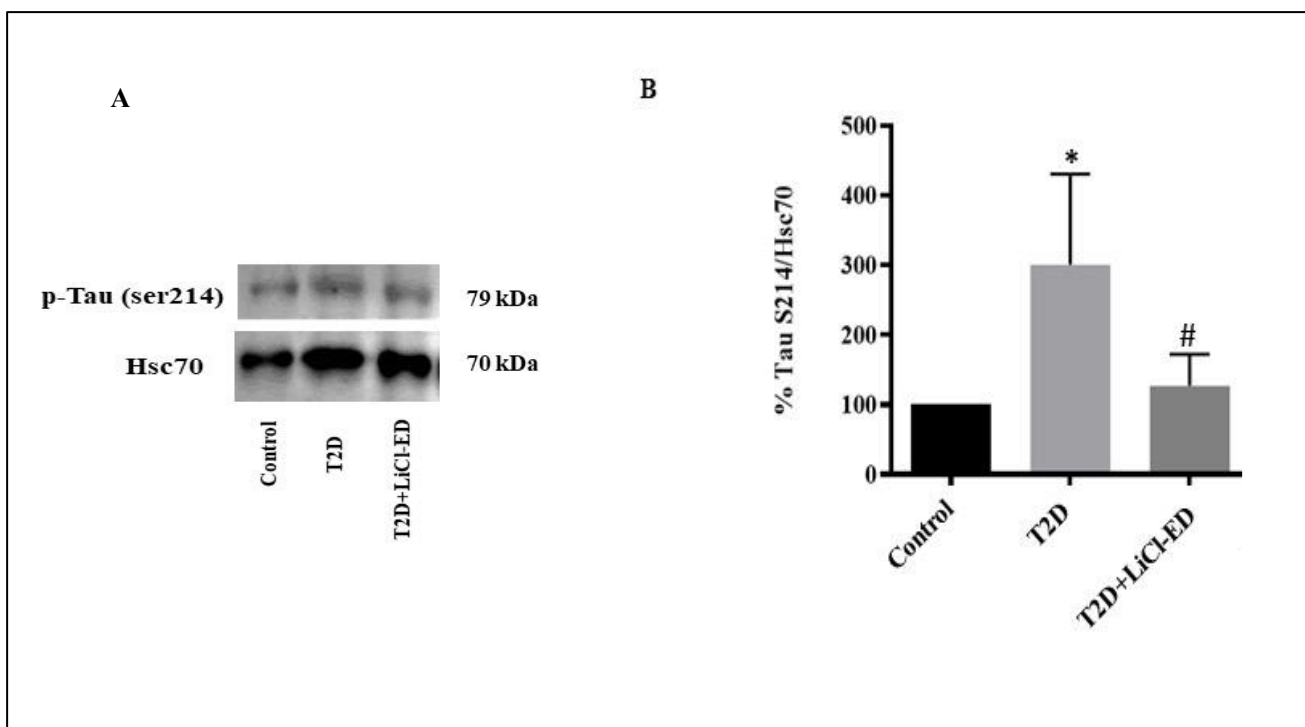


Figure 4: The effect of LiCl on Tau protein hyperphosphorylation in the hearts of T2D rats.

Tau phosphorylation levels in the left ventricles of the three rat groups: control rats, type 2 diabetic rats (T2D), and LiCl HFD T2D rats treated every day (A) Tau protein and Hsc70 levels representative Western blots. (B) histograms showing Western blot quantification. Data are shown as mean \pm SE. n =5 per group.

* $P < 0.05$ vs. control; # $P < 0.05$ vs. diabetic

Regarding the follow up on metabolic parameters of the animal groups, T2D rats had a significant increase in their body weights compared to controls; whereas diabetic group treated with LiCl every day had significant reduction in their body weights as compared to the untreated diabetic rats (Table1). Blood glucose levels were significantly increased in diabetic rats in comparison to their control littermates. Remarkably, there was no significant difference in the blood glucose between the untreated diabetic rats and diabetic rats treated with LiCl (Table1). Following 14 weeks of treatment, rats were sacrificed and the Heart Weight (g) and Tibia length (cm) were measured. The ratio of Heart weight (g) to Tibia Length (cm) and the ratio of Left Ventricular Mass (g) to Tibia Length (cm) were calculated. Ratio of HW/TL (g/cm)

significantly increased in untreated T2D rats, nevertheless it decreased significantly after LiCl treatment. In a similar manner, the ratio of LVM/TL (g/cm) significantly increased in the T2D group compared to the control group; however, it decreased significantly in the group treated with LiCl.

Parameter	Control	T2D	T2D+LiCl-ED
Body Weight (g)	350.10±62.07	456.40±20.59*	347.20±24.82#
Blood Glucose (mg/dl)	114.58±5.81	355.45±22.69*	282.04±40.03*
LVM/TL (g/cm)	0.37±0.06	0.46±0.01*	0.33±0.01#
HW/TL (g/cm)	0.38±0.04	0.53±0.03*	0.37±0.02#

Table 1. Metabolic parameters of the four groups: control rats, T2D rats, and LiCl treated T2D rats. Body weight (g) and blood glucose (mg/dl) were measured weekly across the study for a duration of 18 weeks. Heart weight (HW) (g), tibia length (TL) (cm) and blood glucose levels at the basal fasting state were measured on the sacrifice day of the rats. Left Ventricular Mass (LVM) was measured using the echocardiogram. Values are means ± SE; n = 5 per group.
* $P < 0.05$ vs. control; # $P < 0.05$ vs. diabetic

To evaluate the effect of inhibition of Tau hyperphosphorylation on hyperglycemia-induced cardiac injury, echocardiography analysis was performed. The percentage of LV fractional shortening (%FS) and the LV ejection fraction (%EF) were calculated to assess cardiac function and contractility. Our results show a significant decrease in the %FS in the untreated T2D rats when compared to their controls, which was repaired in the diabetic rats treated with LiCl (**Figure 5A**). In parallel with these

findings, the diabetic animals had a significant decrease in the %EF, which was restored in all the LiCl-treated diabetic rats (**Figure 5B**).

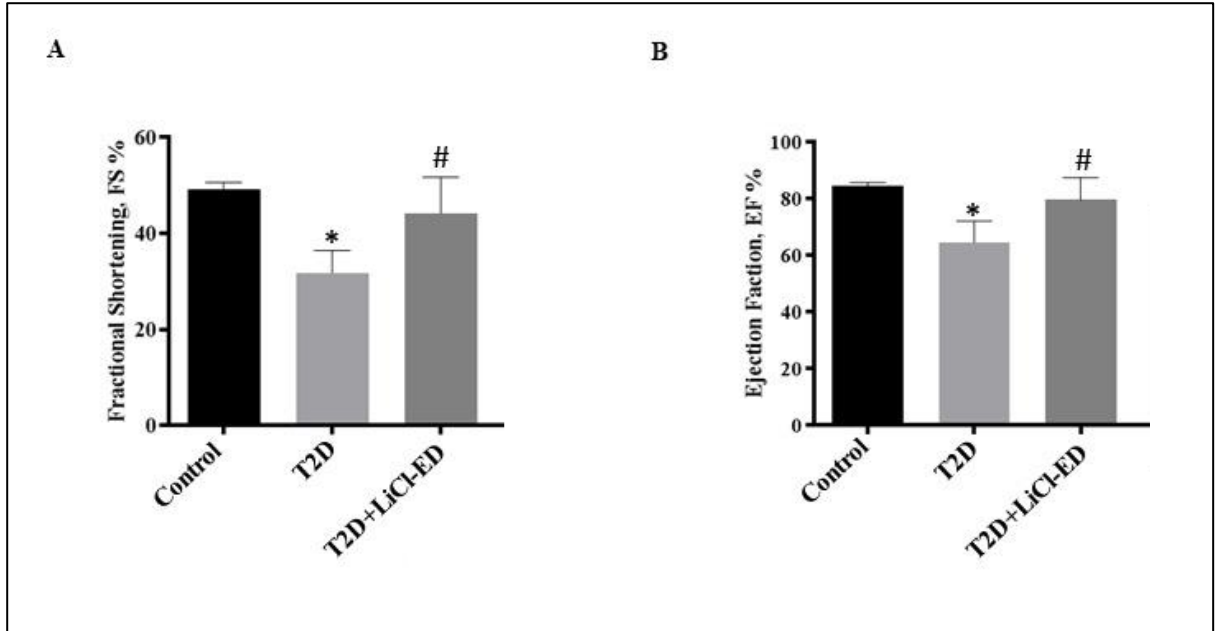


Figure 5: The effect of LiCl on cardiac function.

Echocardiography of the three rat groups: control rats, type 2 diabetic rats (T2D), and LiCl treated type 2 diabetic rats, treated every day for 14 weeks. (A) percentage of fractional shortening FS and (B) percentage of ejection fraction EF. Data are shown as mean \pm SE. n =5 per group.

* $P < 0.05$ vs. control; # $P < 0.05$ vs. diabetic

To further study the effect of LiCl treatment on diabetic animals, histological changes in the LV were assessed. Extracellular matrix macromolecules accumulate as fibrous proteins, collagen, and internal polysaccharides (glycogen) in response to myocardial injury. Masson's Trichrome stain detects collagen deposition, which is considered a major contributor to myocardial fibrosis. Our results show that hyperglycemia induced collagen deposition in the left ventricle tissues of untreated type 2 diabetic rats compared to the control group. Interestingly, the myocardial fibrotic area was reduced significantly after LiCL treatments as compared to untreated diabetic rats with more improvements obtained with everyday treatment of 1mmol/kg LiCl (**Figures 6A**). On the other hand, PAS stain detects glycosylated proteins within the tissue, a

marker of myocardial fibrosis. Our results shows a significant increase in the protein glycosylation in the left ventricle tissues of T2D rats when compared to the control group. Additionally, diabetic rats treated with LiCl show a significant reduction in glycosylation when compared to untreated diabetic rats (**Figures 6B**). Taken together, these results show that LiCl treatment attenuates myocardial fibrosis in type 2 diabetic rats, since it decreases collagen deposition and protein glycosylation in the myocardial tissue.

Collectively, these findings suggest that hyperglycemia-induced cardiac injury in type 2 diabetic animal model is mediated by hyperphosphorylation of Tau protein in the left ventricular tissue.

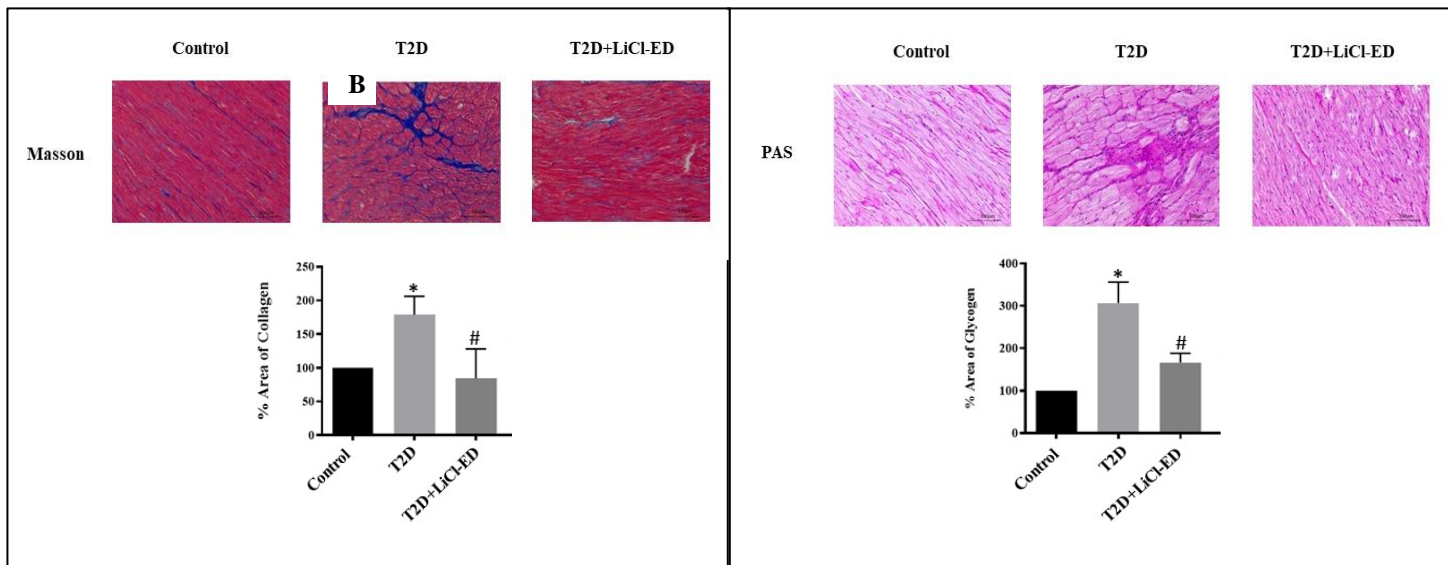


Figure 6: The effect of LiCl on the histology of the LVs in diabetic rats.

Histological analysis of the three rat groups: control rats, type 2 diabetic rats (T2D), and LiCl treated type 2 diabetic rats treated every day 14 weeks. (**A and B**) Representative figure of Masson's trichrome and PAS staining (10X objective) of the left ventricle sections. Histograms showing quantification of the collagen deposition representing highly fibrotic area and of the glycogen deposition intensity representing highly fibrotic areas. Data is shown as mean \pm SE. n =5 per group.

* $P < 0.05$ vs. control; # $P < 0.05$ vs. diabetic

B. Treatment with LiCl attenuates ROS production

Recently accumulating evidence suggest that ROS might be the final common pathway leading to the progression of diabetic complications [81, 82]. To determine if hyperglycemia-induced ROS production is in part responsible for the functional, histopathological, and biochemical changes observed in the left ventricle, ROS was assessed by HPLC. Our HPLC results show that ROS production was significantly increased in the untreated type 2 diabetic rats when compared to the control rats. Remarkably, LiCl treatment significantly restored superoxide levels in treated diabetic rats (**Figure 7**).

These results indicate that the inhibition of tau hyperphosphorylation via LiCl reverse the diabetes-induced increase in ROS production, suggesting a possible interplay between tau hyperphosphorylation and diabetes-induced heart injury.

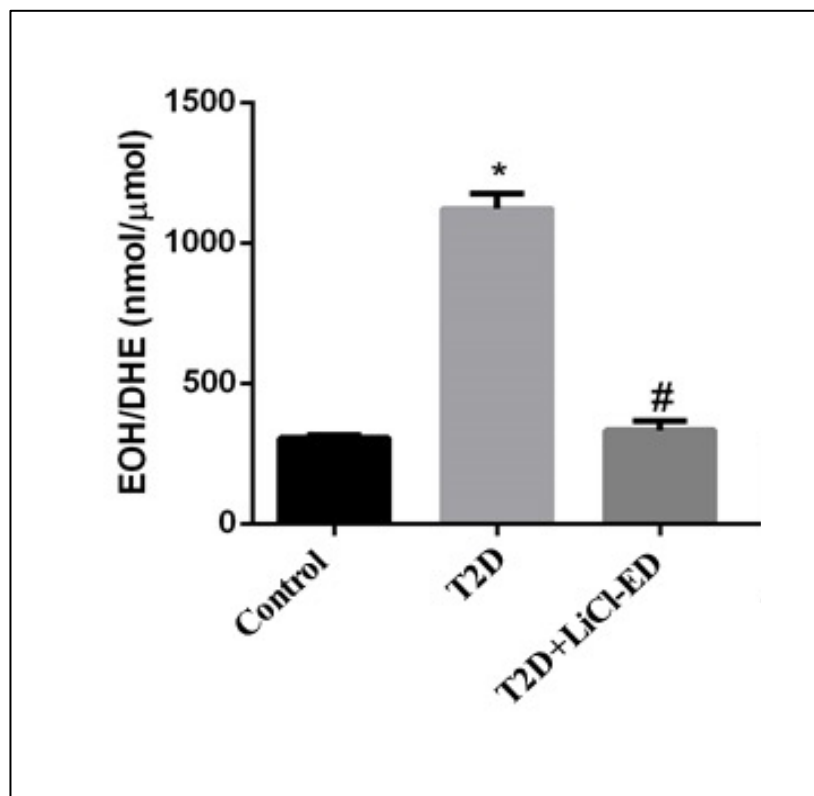


Figure 7: The effect of LiCl on ROS production in the hearts of T2D rats.

Superoxide production in the left ventricles of the three rat groups: control rats, type 2 diabetic rats (T2D), and LiCl type 2 diabetic rats treated every day for 14 weeks. Histogram showing superoxide production using HPLC. Data are shown as mean \pm SE. n =5 per group.

* $P < 0.05$ vs. control; # $P < 0.05$ vs. diabetic

C. Inhibition of 20-HETE regulates diabetes induced cardiac injury

Data from the literature have demonstrated the involvement of CYP families and their metabolites in the production of ROS. Moreover, our group and others have suggested that the alterations in 20-HETE levels induce cardiovascular complications [28, 29, 83-85]. In fact, it is suggested that 20-HETE increase ROS production leading to diabetes-induced heart injury [29]. However, the mechanism of action of 20-HETE is not well elucidated. We hypothesize that 20-HETE, by altering tau hyperphosphorylation and thus its aggregation, increases ROS production. To test our hypothesis, FVB/NJ T2D mice were treated with HET0016, a CYP4A inhibitor, to block 20-HETE production.

At the level of the metabolic parameters, non-treated type 2 diabetic mice exhibited a significant increase in blood glucose levels when compared to the control group treated with HET0016. Notably, type 2 diabetic mice treated with HET0016 showed no significant difference in blood glucose level in comparison to the untreated diabetic group (**Table 2**). Moreover, the index of left ventricular hypertrophy (LVM/TL) did not show a remarkable increase in the untreated T2D mice paralleled to a decrease in the diabetic group treated with HET0016 (**Table 2**). However, these are preliminary findings (n=2), so we need to increase the number of animals to obtain more conclusive results.

Parameter	Control+HET0016	T2D	T2D+HET0016
Body Weight (g)	24.60±0.77	25.75±1.34	23.53±1.55
Blood Glucose (mg/dl)	141±99	263±90	257±47
LVM/TL (mg/mm)	5.51±0.38	9.40±0.04	6.54±0.35

Table 2: Metabolic parameters of the three groups: Control+HET0016, T2D, and T2D+HET0016. Body Weight (g) and Blood Glucose (mg/dl) were measured weekly across the study. Heart weight (HW) (g), tibia length (TL) (cm) and blood glucose levels at the basal fasting state were measured on the sacrifice day of the mice. Left Ventricular Mass (LVM) was measured using the echocardiogram. Values are means ± SE; n=2 per group.

In order to assess the effect of HET0016 treatment on cardiac function, hemodynamics variables of the three mice groups were measured, including LV End Diastolic Diameter (LVEDD), LV End Systolic Diameter (LVESD), LV End Diastolic Volume (LVEDV), and LV End Systolic Volume (LVESV). Subsequently, the percentage of LV Fractional Shortening (%FS) and LV Ejection Fraction (%EF) were measured. Our results show a notable change in %FS and %EF in the untreated diabetic animals, accompanied with a marked increase in the T2D mice treated with HET0016. (**Figures 8A and 8B**).

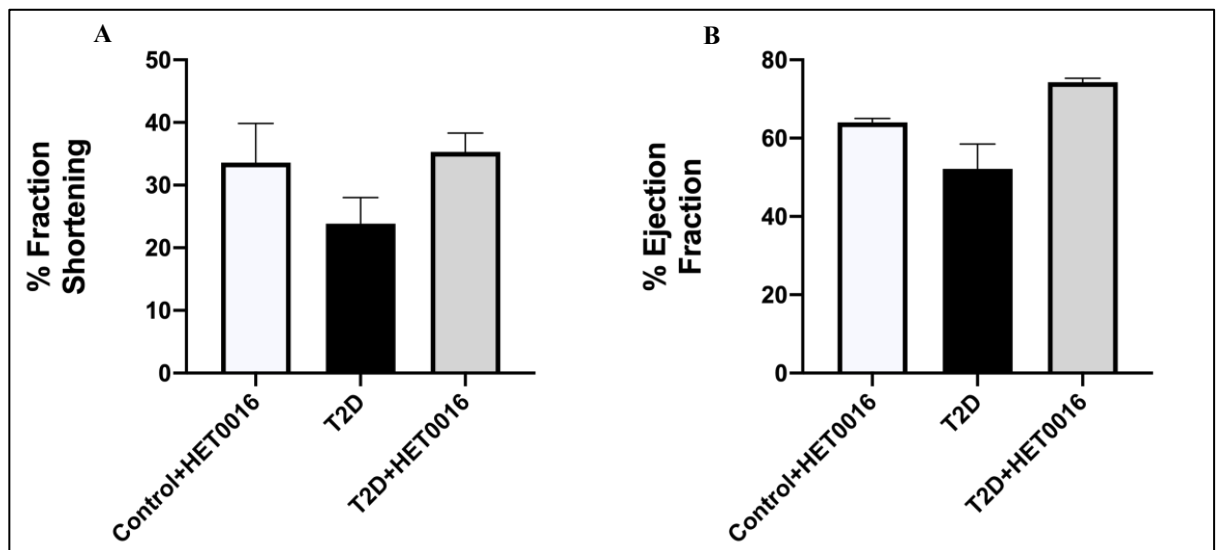


Figure 8: The effect of HET0016 on cardiac function.

Echocardiography of the three mice groups: Control+HET0016, T2D, and T2D+HET0016. (A) percentage of fractional shortening FS and (B) percentage of ejection fraction EF. Data are shown as mean \pm SE. n =2 per group.

As mentioned earlier, Masson's Trichrome stain detects collagen deposition in tissue (blue), while the PAS stain detects glycosylated proteins within the tissue. The Masson's Trichrome representative images indicate more collagen accumulation within the left ventricular section of the untreated type 2 diabetic mice, seen in blue and distinguished from red muscle fibers. This was not seen in the control or diabetic groups treated with HET0016 (**Figure 9**). Additionally, in the PAS stain representative images, we can see more magenta color intensity in the sections of the type 2 diabetic mice compared to the diabetic mice treated with HET0016 and to the treated control group (**Figure 9**).

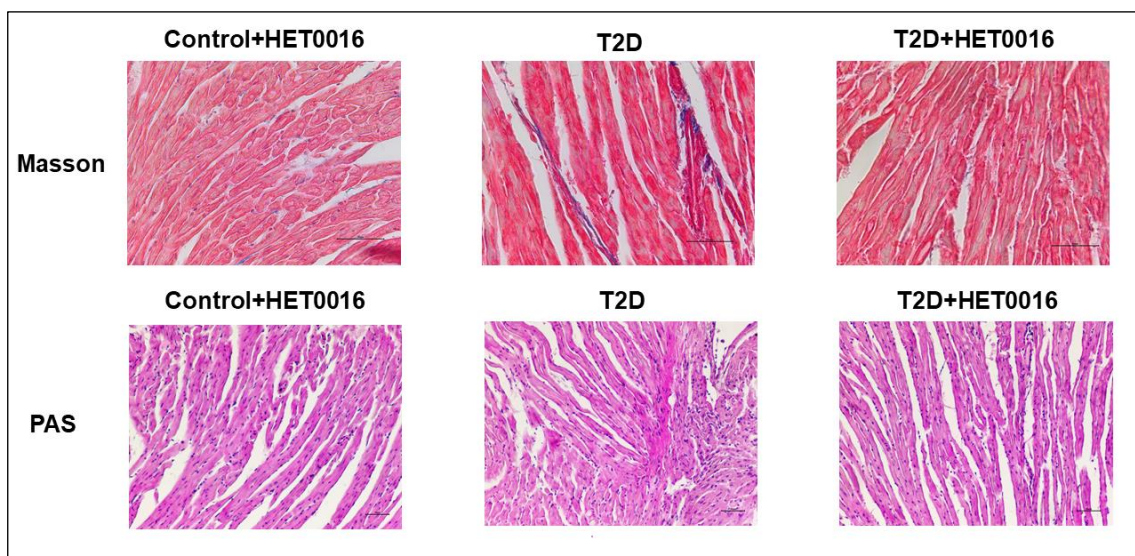


Figure 9: The effect of HET0016 on the histology of the LVs in T2D mice. Representative images of Masson's trichrome and PAS staining (20X objective) of the left ventricle sections of the three mice groups: Control+HET0016, T2D, and T2D+HET0016.

D. Inhibiting 20-HETE production modulates Tau hyperphosphorylation

To determine the consequences of 20-HETE blockade in type 2 diabetes on Tau protein phosphorylation, we explored the expression of p-Tau protein in the left ventricles of the studied mice groups. Western blot analysis results revealed a 60-kDa band of p-Tau S404 showing an increase in the protein expression of p-Tau in the untreated diabetic animals when compared to the control group. This was associated with an obvious decrease in the p-Tau protein levels in the T2D mice treated with HET0016 in comparison to the untreated diabetic mice (**Figures 10A and 10B**). However, as mentioned earlier these are still preliminary results as we have small number of animals per group (n=2), so more animals will be added in the future in order to confirm the effect of 20-HETE on Tau hyperphosphorylation.

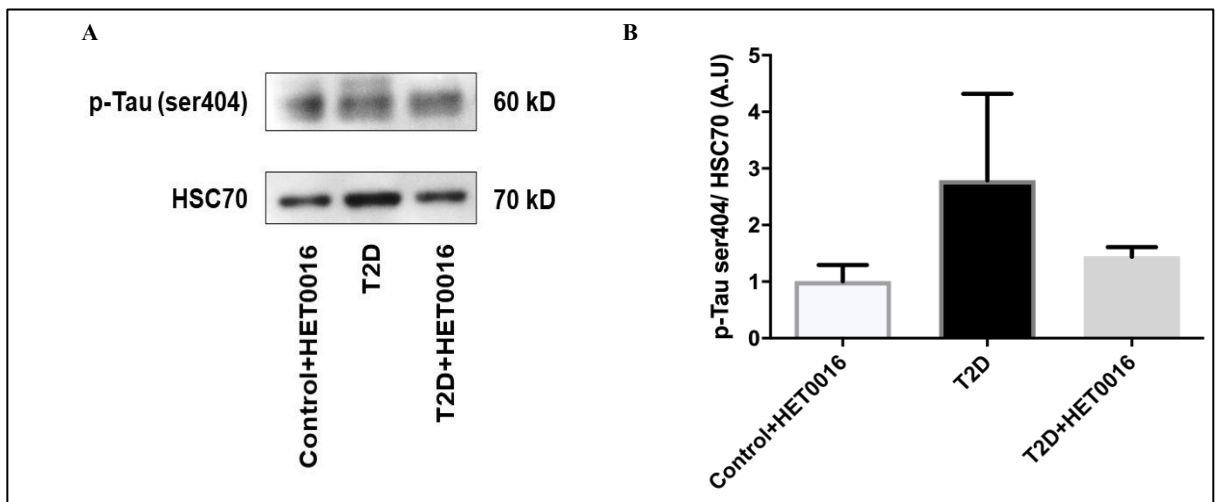


Figure 10: The effect of HET0016 on Tau protein hyperphosphorylation in the hearts of T2D mice. Tau phosphorylation levels in the left ventricles of the three mice groups: Control+HET0016, T2D and T2D+HET0016 (A) p-Tau protein and Hsc70 levels representative Western blots. (B) Histograms showing Western blot quantification. Data are shown as mean \pm SE; n=2 per group

CHAPTER IV

DISCUSSION

Among the most common complications of diabetes, lies diabetic cardiomyopathy, a clinical condition diagnosed with the development of ventricular dysfunction in diabetic patients in the absence of other factors such as hypertension and atherosclerosis. DCM progresses from structural and metabolic abnormalities in the ventricle to overall cardiac remodeling and contractile dysfunction, as well as, extracellular matrix macromolecule accumulation as fibrous proteins (collagen) and internal polysaccharides (glycogen), which eventually leads to heart failure [86, 87].

Tau protein has been highlighted as a new player in a number of diseases, including podocyuria. Eid et al. proposed tau hyperphosphorylation as a novel mechanism involved in podocyte microtubule reorganization, and thus podocyte injury [76]. This opens the possibility of a potential role for tau hyperphosphorylation in cardiac injury. Consequently, for the purpose of exploring the role of tau hyperphosphorylation in the diabetic heart, LiCl, an inhibitor of Glycogen Synthase Kinase-3 (GSK-3), was applied to HFD/STZ-induced type 2 diabetic rats for a period of 14 weeks.

Lithium Chloride treatment has been widely used to prevent tau phosphorylation through GSK-3 β inhibition, mimicking insulin like effects of regulating glucose metabolism, [88-90]. This was seen by a slight decrease in blood glucose level and other parameters mainly after the everyday treatment of LiCl. This supports the effect of lithium on blood glucose level in the T2D rat models treated every day, compared to that of the untreated diabetic models. Furthermore, the body weights of the treated

diabetic group of rats has been shown to decrease significantly compared to the untreated diabetic rats. This further explains the role tau hyperphosphorylation plays in diabetes, which suggests a possible role of GSK-3 β in easing the burdens of diabetes (Table 1).

Moreover, amongst the most important indicators of hypertrophy in the cardiac tissue are the heart weight to tibia length and left ventricular mass to tibia length indices. In our results, heart weight normalized to tibia length indicated a significant increase in the T2D rats as compared to the control group. This ratio was significantly reduced in both diabetic groups treated with 1mmol/kg LiCl, with a more significant reduction observed in the group treated every day. Uniformly, these results coincide with the left ventricular mass to tibia length ratio, whereby we see a significant increase in this ratio in the untreated diabetic groups in comparison to the control group. This ratio is also decreased significantly after the LiCl treatment. These results are presented in Table 1 and confirm that the disease complications will continue to deteriorate with time, providing the characteristics seen upon the development of DCM, including abnormal cellular metabolism, functional and structural alterations of the myocardium, followed by impaired cardiac function [91-93]. Our results might also imply that the hypertrophic character is witnessed mainly in the left ventricular muscle, which is further elucidated by the left ventricular function assessment using an echocardiogram. Our echocardiography measurements indicated a significant decrease in the percent fractional shortening, %FS (Figure 5A) and in the percent ejection fraction, %EF (Figure 5B), in the T2D rat group compared to the control group, which suggests a systolic function impairment. Further, %EF levels were decreased to 65% indicating a heart failure with preserved ejection fraction (>50%). This suggests left ventricular

hypertrophy as a compensatory mechanism undergone in the left ventricles of diabetic rats upon cardiac injury. Therefore, the heart responds by increasing its wall thickness and thus exerting more force to pump blood, which is why we see a preserved ejection fraction for the decreased ejection capacity in the left ventricles. Consistent with our findings, the %FS and %EF were significantly decreased after LiCl treatment in the treated groups (Figures 5A and 5B). These results indicate an attenuation of cardiac injury upon treatment of LiCl, which confirms the findings of other groups, who have shown improved left ventricular molecular functions; in addition to, preventing myocardial injury and apoptosis of cardiomyocytes [94, 95]. Other groups have also shown a cardioprotective effect exhibited by GSK-3 β inhibition via LiCl, as well as a decreased atherosclerosis in HFD mouse models [96, 97].

Moreover, several studies have identified glycogen and collagen deposition as a key hallmark in response to cardiac injury [98, 99]. Myofibroblasts secrete an abundance of collagen and other proteins which accumulate in the extracellular matrix [100]. To detect the accumulation of these molecules, we use Masson's Trichrome stain to detect the collagen deposition and PAS stain to detect glycosylated proteins within the tissue. Histological assessment of these fibrotic changes reflects cardiac dysfunction in diabetes [101]. Our results show that hyperglycemia significantly increased collagen deposition in the left ventricle tissues of type 2 diabetic rats compared to the control group. Of interest, the myocardial fibrotic area was significantly reduced after LiCl treatment compared to the diabetic group (Figures 6A and 6B). This suggests an association between tau hyperphosphorylation and cardiac pathology.

Additionally, to establish Tau protein involvement in the pathogenesis of DCM, and whether LiCl treatment was effective in ameliorating cardiac injury, Tau protein

expression was assessed in the left ventricles of the three rat groups. The results indicated a significant increase in tau phosphorylation in the left ventricles of the type 2 diabetic rats compared to the control. The expression of phospho-Tau significantly decreased after LiCl treatment (Figures 4A and 4B). This suggests an important mechanism of tau protein hyperphosphorylation in diabetes induced cardiac dysfunction. Our results are reinforced by the findings of Planel et al., whereby they showed that insulin deficiency increases GSK-3 β activity, leading to Tau hyperphosphorylation [102]. Adding to that, impaired insulin signaling was linked to pathogenic Tau aggregation in neurons [103]. As for Tau in the heart, KO mice developed increased systolic blood pressure and cardiac hypertrophy at 13 months, which was then followed by a reduction in left atrial contractility at 23 months, indicating an important role for Tau in cardiovascular pathophysiology [78]. Thus, Tau protein hyperphosphorylation appears to be an important mechanism involved in regulating cardiac dysfunction.

Diabetes and oxidative stress are believed to be major players leading to the cardiac functional and structural changes observed in heart injury [104]. Accumulating experimental and clinical evidence propose ROS production as a final common pathway leading to the development of diabetic complications [81, 82]. Aiming to determine if diabetes-induced ROS production is behind the pathological features observed in the left ventricle, we assessed ROS production levels by HPLC. Our results show that ROS production significantly elevated in the T2D rats in comparison to the control group. Remarkably, LiCl treatment and thus inhibition of tau hyperphosphorylation significantly decreased ROS production in the treated groups (Figure 7), suggesting a possible interplay between tau hyperphosphorylation and diabetes-induced heart injury.

CYP450 are reported to be major sources of ROS in numerous tissues [105-109] with major implications in diabetic complications [110, 111]. CYP4A, of the hydroxylase family of CYPs, is known to be present in the heart, vascular smooth muscles, and endothelial cells. Strong evidence suggests that the alteration in the levels of CYP450 and thus its metabolites contribute to the diabetes-induced organ dysfunction. Of interest, the CYP4A metabolite, 20-HETE has been shown to be a major player in heart injury, mainly suggested to play a vasoconstrictive effect on the vasculature and herein, mediating the injury [112, 113]. Our group studied the effect of CYP metabolites on cardiac dysfunction in type 1 diabetic rats, showing an elevated level of 20-HETE in the left ventricles of the diabetic animals. The study also provided evidence that treating with HET0016, hydrolase inhibitor, may have a cardio-protective effect reflected by a decrease in infarct size and apoptosis [114].

Aiming to investigate the interplay between Tau protein hyperphosphorylation and ROS production by the CYP4A subfamily of enzymes, we blocked 20-HETE production using HET0016. The aforementioned beneficial effects on cardiac tissue were further reflected by our results. At the level of metabolic parameters, blood glucose levels of the T2D mice significantly increased compared to the control treated group. This increase was unchanged upon treatment with HET0016. Left ventricular hypertrophy index, represented as the ratio of Left Ventricular Mass to Tibia Length has a tendency to increase in the T2D mice group, despite the fact that number of animals per group needs to be increased, and then tends to decrease in the T2D group treated with HET0016, suggesting a possibility of left ventricular hypertrophy in untreated diabetic mice that was partially reversed in the diabetic group treated with HET0016 (Table 2). At the level of cardiac function, despite the small number of animals (n) per

group, HET0016 shows a tendency to regulate %EF and %FS. Fraction Shortening % tends to decrease slightly in the T2D mice models, however, it tends to increase in the HET0016 treated diabetic group (Figure 8A). A similar trend is seen in the Ejection Fraction %, whereby it tends to decrease in the T2D group as compared to the controls and tends to increase in the T2D+HET0016 group (Figure 8B). At the level of histology, collagen deposition in tissue is detected by Masson's Trichrome stain seen in blue, while the PAS stain detects glycosylated proteins within the tissue. The Masson's Trichrome representative images indicate more collagen accumulation within the left ventricular section of the type 2 diabetic mice, seen in blue and distinguished from red muscle fibers. However, this was not seen in the Control+HET0016 and T2D+HET0016 groups. Furthermore, in the representative images of the PAS stain of the LV sections, we can see more magenta color intensity in the sections of the type 2 diabetic mice compared to those treated with HET0016 and to the treated control group (Figure 9). These findings suggest that 20-HETE blockade may inhibit the myocardial fibrosis of the left ventricle tissue manifested in T2D mice.

Finally, to determine whether the inhibition of 20-HETE is regulating the cardiac function of the treated diabetic mice by modulating Tau hyperphosphorylation levels, Western Blot analysis was performed to measure the expression of p-Tau S404 levels in the three mice groups. Our results indicate a trend whereby Tau hyperphosphorylation levels are increased in T2D mice. Upon treatment with HET0016 and thus blocking 20-HETE production, Tau phosphorylation shows a tendency to decrease (Figure 10). Consequently, we speculate that 20-HETE is upstream of p-Tau, since a decrease in the production of 20-HETE leads to a decrease in p-Tau levels,

suggesting a mechanism of action leading to ROS generation and thereby the progression of DCM.

Taken together, our data suggest that blocking Tau protein hyperphosphorylation via LiCl as a kinase inhibitor and via HET0016, a CYP4A inhibitor, attenuates cardiac injury and is therefore a potential therapeutic target for diabetes-induced cardiac damage. More importantly, we highlight that an increase in 20-HETE production levels induces the observed myocardial damage probably by stimulating ROS overproduction mediated by Tau hyperphosphorylation.

CHAPTER V

LIMITATIONS AND FUTURE PERSPECTIVES

In our study, the small number of animals was the main limiting factor for the molecular experiments. Groups consisted of three to four mice only. Therefore, we will be increasing the number of animals in the future which might provide more significance to our results. Further, we will also assess additional markers of cardiac injury. Other sources of ROS can be investigated in the context of Tau hyperphosphorylation. Also, the effect of inhibiting Tau hyperphosphorylation on 20-HETE levels can be investigated to gain further insights regarding the mechanism of action.

REFERENCES

1. Bugger, H. and E.D. Abel, *Molecular mechanisms of diabetic cardiomyopathy*. *Diabetologia*, 2014. **57**(4): p. 660-71.
2. *Diagnosis and classification of diabetes mellitus*. *Diabetes Care*, 2011. **34 Suppl 1**(Suppl 1): p. S62-9.
3. Henning, R.J., *Type-2 diabetes mellitus and cardiovascular disease*. *Future Cardiol*, 2018. **14**(6): p. 491-509.
4. King, G.L. and M. Brownlee, *The cellular and molecular mechanisms of diabetic complications*. *Endocrinol Metab Clin North Am*, 1996. **25**(2): p. 255-70.
5. Boyle, P.J., *Diabetes mellitus and macrovascular disease: mechanisms and mediators*. *Am J Med*, 2007. **120**(9 Suppl 2): p. S12-7.
6. Litwak, L., et al., *Prevalence of diabetes complications in people with type 2 diabetes mellitus and its association with baseline characteristics in the multinational A1chieve study*. *Diabetol Metab Syndr*, 2013. **5**(1): p. 57.
7. Ceriello, A., *Hyperglycaemia and the vessel wall: the pathophysiological aspects on the atherosclerotic burden in patients with diabetes*. *Eur J Cardiovasc Prev Rehabil*, 2010. **17 Suppl 1**: p. S15-9.
8. Liu, J.E., et al., *The impact of diabetes on left ventricular filling pattern in normotensive and hypertensive adults: the Strong Heart Study*. *J Am Coll Cardiol*, 2001. **37**(7): p. 1943-9.
9. Rutter, M.K., et al., *Impact of glucose intolerance and insulin resistance on cardiac structure and function: sex-related differences in the Framingham Heart Study*. *Circulation*, 2003. **107**(3): p. 448-54.
10. Jia, G., V.G. DeMarco, and J.R. Sowers, *Insulin resistance and hyperinsulinaemia in diabetic cardiomyopathy*. *Nat Rev Endocrinol*, 2016. **12**(3): p. 144-53.
11. Westermeier, F., et al., *New Molecular Insights of Insulin in Diabetic Cardiomyopathy*. *Front Physiol*, 2016. **7**: p. 125.
12. Giam, B., D.M. Kaye, and N.W. Rajapakse, *Role of Renal Oxidative Stress in the Pathogenesis of the Cardiorenal Syndrome*. *Heart Lung Circ*, 2016. **25**(8): p. 874-80.
13. Wallace, D.C., *A mitochondrial paradigm for degenerative diseases and ageing*. *Novartis Found Symp*, 2001. **235**: p. 247-63; discussion 263-6.
14. Fang, Z.Y., J.B. Prins, and T.H. Marwick, *Diabetic cardiomyopathy: evidence, mechanisms, and therapeutic implications*. *Endocr Rev*, 2004. **25**(4): p. 543-67.
15. Cai, L. and Y.J. Kang, *Cell death and diabetic cardiomyopathy*. *Cardiovasc Toxicol*, 2003. **3**(3): p. 219-28.
16. Cai, L. and Y.J. Kang, *Oxidative stress and diabetic cardiomyopathy: a brief review*. *Cardiovasc Toxicol*, 2001. **1**(3): p. 181-93.
17. Diwan, A., et al., *Inflammatory mediators and the failing heart: a translational approach*. *Curr Mol Med*, 2003. **3**(2): p. 161-82.
18. Palomer, X., et al., *An overview of the crosstalk between inflammatory processes and metabolic dysregulation during diabetic cardiomyopathy*. *Int J Cardiol*, 2013. **168**(4): p. 3160-72.
19. Berg, T.J., et al., *Serum levels of advanced glycation end products are associated with left ventricular diastolic function in patients with type 1 diabetes*. *Diabetes Care*, 1999. **22**(7): p. 1186-90.

20. Volpe, C.M.O., et al., *Cellular death, reactive oxygen species (ROS) and diabetic complications*. Cell Death Dis, 2018. **9**(2): p. 119.
21. Ammar, L.A., et al., *Immunomodulatory Approaches in Diabetes-Induced Cardiorenal Syndromes*. Frontiers in Cardiovascular Medicine, 2021. **7**(439).
22. Waring, R.H., *Cytochrome P450: genotype to phenotype*. Xenobiotica, 2020. **50**(1): p. 9-18.
23. Lamb, D.C., et al., *The first virally encoded cytochrome p450*. J Virol, 2009. **83**(16): p. 8266-9.
24. McLean, K.J., et al., *Biodiversity of cytochrome P450 redox systems*. Biochem Soc Trans, 2005. **33**(Pt 4): p. 796-801.
25. Munro, A.W., H.M. Girvan, and K.J. McLean, *Cytochrome P450--redox partner fusion enzymes*. Biochim Biophys Acta, 2007. **1770**(3): p. 345-59.
26. Guengerich, F.P., *Common and uncommon cytochrome P450 reactions related to metabolism and chemical toxicity*. Chem Res Toxicol, 2001. **14**(6): p. 611-50.
27. Roman, R.J., *P-450 metabolites of arachidonic acid in the control of cardiovascular function*. Physiol Rev, 2002. **82**(1): p. 131-85.
28. Rocic, P. and M.L. Schwartzman, *20-HETE in the regulation of vascular and cardiac function*. Pharmacol Ther, 2018. **192**: p. 74-87.
29. Alaeddine, L.M., et al., *Pharmacological regulation of cytochrome P450 metabolites of arachidonic acid attenuates cardiac injury in diabetic rats*. Transl Res, 2021. **235**: p. 85-101.
30. Alsaad, A.M., et al., *Role of cytochrome P450-mediated arachidonic acid metabolites in the pathogenesis of cardiac hypertrophy*. Drug Metab Rev, 2013. **45**(2): p. 173-95.
31. Gottlieb, R.A., *Cytochrome P450: major player in reperfusion injury*. Arch Biochem Biophys, 2003. **420**(2): p. 262-7.
32. Kaludercic, N. and F. Di Lisa, *Mitochondrial ROS Formation in the Pathogenesis of Diabetic Cardiomyopathy*. Front Cardiovasc Med, 2020. **7**: p. 12.
33. Weingarten, M.D., et al., *A protein factor essential for microtubule assembly*. Proc Natl Acad Sci U S A, 1975. **72**(5): p. 1858-62.
34. Goedert, M. and M.G. Spillantini, *A century of Alzheimer's disease*. Science, 2006. **314**(5800): p. 777-81.
35. Feinstein, S.C. and L. Wilson, *Inability of tau to properly regulate neuronal microtubule dynamics: a loss-of-function mechanism by which tau might mediate neuronal cell death*. Biochim Biophys Acta, 2005. **1739**(2-3): p. 268-79.
36. Gu, Y., F. Oyama, and Y. Ihara, *Tau is widely expressed in rat tissues*. J Neurochem, 1996. **67**(3): p. 1235-44.
37. Iqbal, K., et al., *Tau in Alzheimer disease and related tauopathies*. Curr Alzheimer Res, 2010. **7**(8): p. 656-64.
38. Caillet-Boudin, M.L., et al., *Regulation of human MAPT gene expression*. Mol Neurodegener, 2015. **10**: p. 28.
39. Goedert, M., et al., *Multiple isoforms of human microtubule-associated protein tau: sequences and localization in neurofibrillary tangles of Alzheimer's disease*. Neuron, 1989. **3**(4): p. 519-26.
40. Sergeant, N., A. Delacourte, and L. Buée, *Tau protein as a differential biomarker of tauopathies*. Biochim Biophys Acta, 2005. **1739**(2-3): p. 179-97.
41. Couchie, D., et al., *Primary structure of high molecular weight tau present in the peripheral nervous system*. Proc Natl Acad Sci U S A, 1992. **89**(10): p. 4378-81.

42. Andreadis, A., W.M. Brown, and K.S. Kosik, *Structure and novel exons of the human tau gene*. *Biochemistry*, 1992. **31**(43): p. 10626-33.
43. King, M.E., et al., *Differential assembly of human tau isoforms in the presence of arachidonic acid*. *J Neurochem*, 2000. **74**(4): p. 1749-57.
44. Lu, M. and K.S. Kosik, *Competition for microtubule-binding with dual expression of tau missense and splice isoforms*. *Mol Biol Cell*, 2001. **12**(1): p. 171-84.
45. Hirokawa, N., Y. Shiomura, and S. Okabe, *Tau proteins: the molecular structure and mode of binding on microtubules*. *J Cell Biol*, 1988. **107**(4): p. 1449-59.
46. Avila, J., et al., *Role of tau protein in both physiological and pathological conditions*. *Physiol Rev*, 2004. **84**(2): p. 361-84.
47. Popov, K.I., et al., *Insight into the Structure of the "Unstructured" Tau Protein*. *Structure*, 2019. **27**(11): p. 1710-1715.e4.
48. Preuss, U., et al., *The 'jaws' model of tau-microtubule interaction examined in CHO cells*. *J Cell Sci*, 1997. **110 (Pt 6)**: p. 789-800.
49. Matsumoto, S.E., et al., *The twenty-four KDa C-terminal tau fragment increases with aging in tauopathy mice: implications of prion-like properties*. *Hum Mol Genet*, 2015. **24**(22): p. 6403-16.
50. Lee, G., et al., *Tau interacts with src-family non-receptor tyrosine kinases*. *J Cell Sci*, 1998. **111 (Pt 21)**: p. 3167-77.
51. Lau, D.H., et al., *Critical residues involved in tau binding to fyn: implications for tau phosphorylation in Alzheimer's disease*. *Acta Neuropathol Commun*, 2016. **4**(1): p. 49.
52. Jeganathan, S., et al., *Global hairpin folding of tau in solution*. *Biochemistry*, 2006. **45**(7): p. 2283-93.
53. Barbier, P., et al., *Role of Tau as a Microtubule-Associated Protein: Structural and Functional Aspects*. *Front Aging Neurosci*, 2019. **11**: p. 204.
54. Elie, A., et al., *Tau co-organizes dynamic microtubule and actin networks*. *Sci Rep*, 2015. **5**: p. 9964.
55. Stamer, K., et al., *Tau blocks traffic of organelles, neurofilaments, and APP vesicles in neurons and enhances oxidative stress*. *J Cell Biol*, 2002. **156**(6): p. 1051-63.
56. Liao, H., et al., *Protein phosphatase 1 is targeted to microtubules by the microtubule-associated protein Tau*. *J Biol Chem*, 1998. **273**(34): p. 21901-8.
57. Li, H.L., et al., *Phosphorylation of tau antagonizes apoptosis by stabilizing beta-catenin, a mechanism involved in Alzheimer's neurodegeneration*. *Proc Natl Acad Sci U S A*, 2007. **104**(9): p. 3591-6.
58. Violet, M., et al., *A major role for Tau in neuronal DNA and RNA protection in vivo under physiological and hyperthermic conditions*. *Front Cell Neurosci*, 2014. **8**: p. 84.
59. Wolfe, M.S., *The role of tau in neurodegenerative diseases and its potential as a therapeutic target*. *Scientifica (Cairo)*, 2012. **2012**: p. 796024.
60. Ittner, L.M., et al., *Dendritic function of tau mediates amyloid-beta toxicity in Alzheimer's disease mouse models*. *Cell*, 2010. **142**(3): p. 387-97.
61. Lei, P., et al., *Tau deficiency induces parkinsonism with dementia by impairing APP-mediated iron export*. *Nat Med*, 2012. **18**(2): p. 291-5.
62. Morris, M., et al., *Tau post-translational modifications in wild-type and human amyloid precursor protein transgenic mice*. *Nat Neurosci*, 2015. **18**(8): p. 1183-9.

63. Hanger, D.P., B.H. Anderton, and W. Noble, *Tau phosphorylation: the therapeutic challenge for neurodegenerative disease*. Trends Mol Med, 2009. **15**(3): p. 112-9.
64. Drewes, G., et al., *Microtubule-associated protein/microtubule affinity-regulating kinase (p110mark). A novel protein kinase that regulates tau-microtubule interactions and dynamic instability by phosphorylation at the Alzheimer-specific site serine 262*. J Biol Chem, 1995. **270**(13): p. 7679-88.
65. Sadik, G., et al., *Phosphorylation of tau at Ser214 mediates its interaction with 14-3-3 protein: implications for the mechanism of tau aggregation*. J Neurochem, 2009. **108**(1): p. 33-43.
66. Köpke, E., et al., *Microtubule-associated protein tau. Abnormal phosphorylation of a non-paired helical filament pool in Alzheimer disease*. J Biol Chem, 1993. **268**(32): p. 24374-84.
67. Hoover, B.R., et al., *Tau mislocalization to dendritic spines mediates synaptic dysfunction independently of neurodegeneration*. Neuron, 2010. **68**(6): p. 1067-81.
68. Kovacs, G.G., *Tauopathies*. Handb Clin Neurol, 2017. **145**: p. 355-368.
69. Yoshiyama, Y., V.M. Lee, and J.Q. Trojanowski, *Therapeutic strategies for tau mediated neurodegeneration*. J Neurol Neurosurg Psychiatry, 2013. **84**(7): p. 784-95.
70. Mattson, M.P., *Pathways towards and away from Alzheimer's disease*. Nature, 2004. **430**(7000): p. 631-9.
71. Delacourte, A. and A. Defossez, *Alzheimer's disease: Tau proteins, the promoting factors of microtubule assembly, are major components of paired helical filaments*. J Neurol Sci, 1986. **76**(2-3): p. 173-86.
72. García-Sierra, F., S. Mondragón-Rodríguez, and G. Basurto-Islas, *Truncation of tau protein and its pathological significance in Alzheimer's disease*. J Alzheimers Dis, 2008. **14**(4): p. 401-9.
73. Takashima, A., *Tauopathies and tau oligomers*. J Alzheimers Dis, 2013. **37**(3): p. 565-8.
74. Giacobini, E. and G. Gold, *Alzheimer disease therapy--moving from amyloid- β to tau*. Nat Rev Neurol, 2013. **9**(12): p. 677-86.
75. Müller, R., et al., *Expression of microtubule-associated proteins MAP2 and tau in cultured rat brain oligodendrocytes*. Cell Tissue Res, 1997. **288**(2): p. 239-49.
76. Abdallah, M.S., et al., *Transforming growth factor- β 1 and phosphatases modulate COX-2 protein expression and TAU phosphorylation in cultured immortalized podocytes*. Inflamm Res, 2018. **67**(2): p. 191-201.
77. Shults, N.V., et al., *Tau protein in smooth muscle cells and tissues*. bioRxiv, 2020: p. 2020.10.15.341867.
78. Betrie, A.H., et al., *Evidence of a Cardiovascular Function for Microtubule-Associated Protein Tau*. J Alzheimers Dis, 2017. **56**(2): p. 849-860.
79. Rajalingam, S., et al., *Deletion of the Microtubule-associated protein tau (Mapt^{-/-}) results in diastolic heart failure and altered skeletal muscle function in vivo*. The FASEB Journal, 2020. **34**(S1): p. 1-1.
80. Trujillo, A.S., et al., *Exploration and Suppression of Tau-Induced Cardiac and Skeletal Muscle Defects in a Drosophila Model*. Biophysical Journal, 2013. **104**(2): p. 486a.

81. Jay, D., H. Hitomi, and K.K. Griendling, *Oxidative stress and diabetic cardiovascular complications*. Free Radic Biol Med, 2006. **40**(2): p. 183-92.
82. D'Autreaux, B. and M.B. Toledano, *ROS as signalling molecules: mechanisms that generate specificity in ROS homeostasis*. Nat Rev Mol Cell Biol, 2007. **8**(10): p. 813-24.
83. Hoopes, S.L., et al., *Vascular actions of 20-HETE*. Prostaglandins Other Lipid Mediat, 2015. **120**: p. 9-16.
84. Bellien, J. and R. Joannides, *Epoxyeicosatrienoic acid pathway in human health and diseases*. J Cardiovasc Pharmacol, 2013. **61**(3): p. 188-96.
85. Yousef, M.I., A.A. Saad, and L.K. El-Shennawy, *Protective effect of grape seed proanthocyanidin extract against oxidative stress induced by cisplatin in rats*. Food Chem Toxicol, 2009. **47**(6): p. 1176-1183.
86. Tayel, D.I., N.A. El-Sayed, and N.A. El-Sayed, *Dietary pattern and blood pressure levels of adolescents in Sohag, Egypt*. J Egypt Public Health Assoc, 2013. **88**(2): p. 97-103.
87. Cagalinec, M., et al., *Morphology and contractility of cardiac myocytes in early stages of streptozotocin-induced diabetes mellitus in rats*. Physiol Res, 2013. **62**(5): p. 489-501.
88. Davies, S.P., et al., *Specificity and mechanism of action of some commonly used protein kinase inhibitors*. Biochem J, 2000. **351**(Pt 1): p. 95-105.
89. Hermida, O.G., et al., *Effect of lithium on plasma glucose, insulin and glucagon in normal and streptozotocin-diabetic rats: role of glucagon in the hyperglycaemic response*. Br J Pharmacol, 1994. **111**(3): p. 861-5.
90. Nikoulina, S.E., et al., *Inhibition of glycogen synthase kinase 3 improves insulin action and glucose metabolism in human skeletal muscle*. Diabetes, 2002. **51**(7): p. 2190-8.
91. Lee, W.S. and J. Kim, *Diabetic cardiomyopathy: where we are and where we are going*. Korean J Intern Med, 2017. **32**(3): p. 404-421.
92. Sun, L., et al., *Current advances in the study of diabetic cardiomyopathy: From clinicopathological features to molecular therapeutics (Review)*. Mol Med Rep, 2019. **20**(3): p. 2051-2062.
93. Calligaris, S.D., et al., *Mice long-term high-fat diet feeding recapitulates human cardiovascular alterations: an animal model to study the early phases of diabetic cardiomyopathy*. PLoS One, 2013. **8**(4): p. e60931.
94. Hamstra, S.I., et al., *Low-dose lithium feeding increases the SERCA2a-to-phospholamban ratio, improving SERCA function in murine left ventricles*. Exp Physiol, 2020. **105**(4): p. 666-675.
95. Wu, W., X. Liu, and L. Han, *Apoptosis of cardiomyocytes in diabetic cardiomyopathy involves overexpression of glycogen synthase kinase-3 β* . Biosci Rep, 2019. **39**(1).
96. Yadav, H.N., M. Singh, and P.L. Sharma, *Involvement of GSK-3 β in attenuation of the cardioprotective effect of ischemic preconditioning in diabetic rat heart*. Mol Cell Biochem, 2010. **343**(1-2): p. 75-81.
97. Choi, S.E., et al., *Atherosclerosis induced by a high-fat diet is alleviated by lithium chloride via reduction of VCAM expression in ApoE-deficient mice*. Vascul Pharmacol, 2010. **53**(5-6): p. 264-72.

98. Shearer, J., et al., *Exercise training does not correct abnormal cardiac glycogen accumulation in the db/db mouse model of type 2 diabetes*. Am J Physiol Endocrinol Metab, 2011. **301**(1): p. E31-9.
99. Lajoie, C., et al., *Exercise training attenuated the PKB and GSK-3 dephosphorylation in the myocardium of ZDF rats*. J Appl Physiol (1985), 2004. **96**(5): p. 1606-12.
100. Li, C.J., et al., *Cardiac fibrosis and dysfunction in experimental diabetic cardiomyopathy are ameliorated by alpha-lipoic acid*. Cardiovasc Diabetol, 2012. **11**: p. 73.
101. Yan, S.F., R. Ramasamy, and A.M. Schmidt, *Receptor for AGE (RAGE) and its ligands-cast into leading roles in diabetes and the inflammatory response*. J Mol Med (Berl), 2009. **87**(3): p. 235-47.
102. Planel, E., et al., *Insulin dysfunction induces in vivo tau hyperphosphorylation through distinct mechanisms*. J Neurosci, 2007. **27**(50): p. 13635-48.
103. Yarchoan, M., et al., *Abnormal serine phosphorylation of insulin receptor substrate 1 is associated with tau pathology in Alzheimer's disease and tauopathies*. Acta Neuropathol, 2014. **128**(5): p. 679-89.
104. Kakiuchi-Kiyota, S., et al., *Comparison of hepatic transcription profiles of locked ribonucleic acid antisense oligonucleotides: evidence of distinct pathways contributing to non-target mediated toxicity in mice*. Toxicol Sci, 2014. **138**(1): p. 234-48.
105. Bondy, S.C. and S. Naderi, *Contribution of hepatic cytochrome P450 systems to the generation of reactive oxygen species*. Biochem Pharmacol, 1994. **48**(1): p. 155-9.
106. Puntarulo, S. and A.I. Cederbaum, *Production of reactive oxygen species by microsomes enriched in specific human cytochrome P450 enzymes*. Free Radic Biol Med, 1998. **24**(7-8): p. 1324-30.
107. Boulter, C., et al., *Cardiovascular, skeletal, and renal defects in mice with a targeted disruption of the Pkd1 gene*. Proc Natl Acad Sci U S A, 2001. **98**(21): p. 12174-9.
108. Dunn, K.M., et al., *Elevated production of 20-HETE in the cerebral vasculature contributes to severity of ischemic stroke and oxidative stress in spontaneously hypertensive rats*. Am J Physiol Heart Circ Physiol, 2008. **295**(6): p. H2455-65.
109. Medhora, M., et al., *20-HETE increases superoxide production and activates NADPH oxidase in pulmonary artery endothelial cells*. Am J Physiol Lung Cell Mol Physiol, 2008. **294**(5): p. L902-11.
110. Eid, A.A., et al., *Mechanisms of podocyte injury in diabetes: role of cytochrome P450 and NADPH oxidases*. Diabetes, 2009. **58**(5): p. 1201-11.
111. Eid, S., et al., *Involvement of renal cytochromes P450 and arachidonic acid metabolites in diabetic nephropathy*. J Biol Regul Homeost Agents, 2013. **27**(3): p. 693-703.
112. Faulkner, J., et al., *Inhibition of 12/15-Lipoxygenase Reduces Renal Inflammation and Injury in Streptozotocin-Induced Diabetic Mice*. J Diabetes Metab, 2015. **6**(6).
113. Campbell, W.B. and I. Fleming, *Epoxyeicosatrienoic acids and endothelium-dependent responses*. Pflugers Arch, 2010. **459**(6): p. 881-95.
114. Yousif, M.H., I.F. Benter, and R.J. Roman, *Cytochrome P450 metabolites of arachidonic acid play a role in the enhanced cardiac dysfunction in diabetic rats*

following ischaemic reperfusion injury. Auton Autacoid Pharmacol, 2009. **29**(1-2): p. 33-41.